Deletions in the NF-κB pathway as drivers of resistance in Multiple Myeloma

**Deletions of BIRC2, BIRC3, CYLD and TRAF3
and their role in relapse**

Minor research project
Jacqueline Anne Jansen

Under the supervision of
**Yuen Lam Dora Ng &
Jan Krönke**

Department of
Hematology, Oncology
and Tumorimmunology
Charité
Universitätsmedizin Berlin

Laymans summary

Multiple myeloma is a cancer of the blood. Plasma cells, a specific subtype of the white blood cells which usually help you fight infection, become overgrown in the bone marrow and leave no room for healthy blood cells. Although there are many forms of therapy to fight this disease, it still remains incurable due to acquired drug resistance over time. To understand what drives this sudden resistance, and how the cancer cells are eventually able to evade treatment, we searched literature for mutations in the DNA that are correlated to patients who relapse, patients who have a worse overall survival, and patients who have worse progression free survival. These mutations are not often seen in patients at diagnosis, but pop up when patients relapse. Among these, we found some deletions of genes that are involved in a very important pathway within our cells, namely the NF-κB pathway. This pathway consists of a complex network of proteins, responsible for cellular processes such as apoptosis, differentiation, proliferation and immune and stress responses. Deletions of genes in this pathway that can be associated to multiple myeloma relapse are *BIRC2* (also called cIAP1), *BIRC3* (also called cIAP2), *CYLD* and *TRAF3* deletions. We investigated whether deletions of these genes could cause increased drug resistance to two major drugs that are frequently used in the clinic: dexamethasone and pomalidomide. We introduced the deletions into multiple myeloma cell lines, and then tested them for sensitivity to these drugs. We found that upon deletion of *BIRC2*, *BIRC3*, *CYLD* or *TRAF3*, cells became more resistant to both pomalidomide and dexamethasone. In the absence of drug treatment, these cells were not able to proliferate faster than cells without these deletions, but the deletions gave cells an advantage when they were put under drug treatment. Lack of a selective advantage in the absence of treatment is a possible explanation for the fact that these deletions are not common in newly diagnosed patients, but are seen more often in patients who relapse. Deletion of *XIAP*, which so far has not been associated to multiple myeloma relapse but acts in the same pathways, was also able to cause increased resistance to pomalidomide and dexamethasone in our experiments. This might indicate that instead of a gene-specific reaction, increased resistance might be due to alteration of the NF-κB pathway in general. Furthermore, we investigated how these deletions could possibly cause resistance to pomalidomide. We tested the protein levels of one target of pomalidomide, IKZF1, a transcription factor which is very important for plasma cells. When *BIRC2*, *BIRC3*, *CYLD* or *TRAF3* was deleted, we saw higher protein levels of IKZF1 in these cells. This could be an explanation for the observation that these cells became more resistant to pomalidomide: because the target of pomalidomide is present at higher levels at baseline, the drug may not be able to induce complete degradation of the target. With the application of a chemical compound that is able to degrade cIAP1 (the protein name for *BIRC2*), we found that different markers of the NF-κB pathway went up, indicating that when cIAP1 is not present, this pathway becomes more active. In conclusion, we show that deletions of *BIRC2*, *BIRC3*, *CYLD* and *TRAF3* result in a higher resistance to certain forms of therapy, and that this may not be solely a gene-specific phenomenon, but rather a result of alteration of proteins involved in the NF-κB pathway in general. This insight may help to design future therapeutic strategies to overcome resistance in this still incurable disease.

Table of contents:

Abstract

Multiple myeloma is a disease for which various treatment options are available. However, during follow-up virtually all patients relapse due to acquired drug resistance. To elucidate which genetic lesions are at the root of this resistance, we investigated the effects of *BIRC2*/cIAP1, *BIRC3*/cIAP2, *CYLD* and *TRAF3* deletions on resistance to pomalidomide and dexamethasone. These genes are involved in the NF-κB pathway, and their deletion is known to be associated to poor prognosis and worse overall progression free survival. Using CRISPR/Cas9, we created *BIRC2*, *BIRC3*, *CYLD* and *TRAF3* depleted cells and tested their sensitivity to pomalidomide, dexamethasone and combinatory treatment. We found that deletion of any of these genes caused increased resistance to both therapies individually, and also combined. Deletion of *XIAP*, a protein involved in the same pathways but hitherto not associated to poor overall survival, was also able to evoke resistance. This might indicate that instead of a gene-specific reaction, increased resistance might be installed to alteration of the NF-κB pathway in general. *BIRC2*, *BIRC3*, *CYLD* and *TRAF3* deletions caused upregulation of IKZF1 protein levels. Since IKZF1 is a degradation target of pomalidomide, this may explain why these deletions cause drug resistance to pomalidomide. Our results reveal a so-far unreported resistance mechanism to pomalidomide. With the help of transient knock-down of cIAP1, we showed that upregulation of IKZF1 was universal across various multiple myeloma cell lines, and that this upregulation was reversible when cIAP1 levels were restored. We also showed that upon cIAP1 degradation, p65, p100 and p52 protein levels, markers of NF-κB pathway activity, were elevated. RT-qPCR analysis showed that upregulation of IKZF1, p65, p100 and IKZF3 in the absence of cIAP1 was regulated at a transcriptional level. Taken together, these results show that deletions of *BIRC2*, *BIRC3*, *CYLD* and *TRAF3* are drivers of therapy resistance, and highlights the importance of investigating possible sensitivity of cells harboring these deletions to alternate forms of therapy.

Introduction:

Multiple myeloma (MM) is a genetically heterogenous malignancy which is characterized by abnormal proliferation of plasma cells within the bone marrow (Dutta *et al.,* 2022). Although many forms of therapy exist, the disease remains incurable due to acquired drug resistance over time (Kumar *et al.,* 2004). One explanation for this acquired drug resistance is the emergence of drug resistant clones carrying resistance-driving genetic lesions. High somatic mutational load is correlated with reduced progression free survival (Miller *et al.,* 2017). To elucidate which genetic mutations may drive drug resistance, research has been focused on genetic mutations that are specifically enriched in relapse patients and genes that can be associated with poor prognosis and worse overall progression free survival. Among these are deletions of *BIRC2*, *BIRC3*, *TRAF3* and *CYLD*. These genes are involved in the NF-κB pathway (van Andel *et al.,* 2016; Chavan *et al.,* 2017; Keats *et al.,* 2012; Shah *et al.,* 2017). Whether these deletions are solely responsible for drug resistance, and whether they associate with multi-drug resistance remains to be investigated.

The NF-κB pathway and its role in MM

The NF-κB pathway has many activating stimuli and target genes, and serves critical functions in fundamental cellular processes such as apoptosis, differentiation and development, proliferation and immune and stress responses (Hayden and Ghosh 2012; Karin 2006). The NF-κB pathway can be subdivided into the canonical and the non-canonical pathway.

Canonical signaling is brief and responses are restricted by autoregulatory feedback mechanisms. When this pathway is active, IKK (IκB kinase) is able to phosphorylate several inhibitors of the canonical pathway, leading to their degradation. Upon degradation of these inhibitors, p50/p65 heterodimers and c-rel/p65 accumulate in the nucleus and act as transcription factors for NF-κB target genes (Xiao *et al.,* 2001; Annunziata *et al.,* 2007). The canonical signaling is important for enhancement of proliferation and survival of cells. One of the important negative regulators of this pathway is CYLD (Demchenko *et al.,* 2010).

Contrary to the canonical signaling, non-canonical signaling generally sets a delayed and continuous response in motion (Sun, 2010; Nagel *et al.,* 2014). Upon stimulation of this pathway NIK (NF-κB-inducing kinase) activates IKK. IKK in turn phosphorylates p100/NFKB2. Phosphorylation of this unit results in the removal of its inhibitory domain. This again results in the transcription of NF-κB target genes (Xiao *et al.,* 2001; Senftleben *et al.,* 2001). The non-canonical signaling is important for lymphoid development and B-cell maturation (Dejardin, 2006). Control of NIK turnover seems to be a critical step in the activation of this pathway, which is regulated by TRAF3, cIAP1 and cIAP2 (Demchenko *et al.,* 2010). cIAP1 and cIAP2 are the protein names for *BIRC2* and *BIRC3* respectively.

When altered, the NF-κB pathway also has a role in the development and progression of many cancers. Since B-lymphocytes are dependent on NF-κB activation during development, maturation and activation, it is no surprise that constitutive NF-κB activation is seen frequently in lymphoid malignancies including MM (Migliazza *et al.,* 1994; Sun, 2010; Nagel *et al.,* 2014). In MM, mutations leading to the activation of both the canonical and non-canonical NF-κB signaling can be found (Annunziata *et al.,* 2007; Keats *et al.,* 2007). Magrangeas *et al.,* (2013) reported that relapse-acquired mutations targeting NF-κB regulators, and therefore activation of the NF-κB pathway, could potentially contribute to relapse mechanisms in MM. These mutations possibly could include genetic alterations of *BIRC2*, *BIRC3*, *CYLD* and *TRAF3*, which are linked to elevated NF-κB target gene expression (Annunziata *et al.,* 2007).

Inhibitor of apoptosis proteins (IAPs)

cIAP1 and cIAP2 are members of the IAP (inhibitor of apoptosis protein)-family. The genes encoding these proteins, *BIRC2* and *BIRC3,* are both found on chromosome 11 (UniProt Q1390 and Q13489). As their name indicates, these proteins play a critical role as negative regulators of caspases and cell death, but they are also involved in the NF-κB pathway and have a role in cell motility and mitosis (Silke *et al.,* 2013). IAP proteins are defined by the presence of a baculovirus IAP repeat (BIR) domain. This zinc-binding protein-fold is critical for the ability to form protein-protein interactions (Hinds *et al.,* 1999). IAPs have a function as E3-ligases. They are able to ubiquitinate proteins and target them for degradation. The domain critical for this function is the RING domain. IAPs are furthermore not only able to ubiquitinate other proteins, but can also auto-ubiquitinate themselves, leading to their own degradation (Yang *et al.,* 2000). This auto-ubiquitination is thought to be a key process in the apoptotic program.

The ubiquitinating ability of IAPs is important in regard to their role in the NF-κB pathway. cIAP1 and cIAP2 activate RIP1, by mediating K-63 polyubiquitination of RIP1. In turn, RIP1 is able to activate the IKK complex, resulting in activation of the canonical NF-κB pathway (Varfolomeev *et al.,* 2008). K-63 polyubiquitination of RIP1 also represses formation of the pro-apoptotic complex and caspase 8 activity, thereby suppressing apoptosis (Wang *et al.,* 1998).

In contrast, cIAP1 and cIAP2 also have a role in repressing the non-canonical signaling by ubiquitinating NIK. This is done with the help of TRAF2 and TRAF3. As a result of its ubiquitination, NIK is degraded and therefore not able to activate the IKK complex. As a result, non-canonical signaling is suppressed (Liao et al., 2004; Zarnegar et al., 2008). Consequently to these various functions in apoptosis and NF-κB signaling, both a loss and overexpression of cIAP1 and cIAP2 can contribute to tumorigenesis (Lau et al., 2012; Keats et al., 2007; Annunziata et al., 2007). Deletion of both *BIRC2* and *BIRC3* in MM cell lines is associated with accumulation of TRAF3 and NIK, and constant activation of the non-canonical NF-κB pathway (Annunziata et al., 2007, Keats et al., 2007). Homozygous deletion of *BIRC3* was shown to be enriched in relapse patients (Chavan *et al.,* 2017). In a study of Keats et al., (2012) clonal analysis of tumor outgrowth after treatment within MM patients showed outgrowth of clones characterized by a *BIRC2/BIRC3*-deletion (Keats et al., 2012). Moreover, *BIRC2/BIRC3* deletion was shown to be associated with a t(4;14) translocation. This translocation is correlated to poor prognosis and poor overall survival (Shah *et al.,* 2017). Their possible role in resistance remains unclear.

XIAP is another member of the IAP-family, known to be a potent regulator of the apoptotic pathway, whilst also having a role in the NF-κB pathway (Desplanques *et al.,* 2009; Galbán S and Duckett, 2010). *XIAP* downregulation or deletion is not known to be associated to aggressive disease. Rather, XIAP is actually considered a target for promoting cancer cell death, and knock down of *XIAP* results in enhanced drug sensitivity (Desplanques *et al.,* 2009). It remains unknown what the effect of a *BIRC2, BIRC3, CYLD* or *TRAF3* deletion is on drug sensitivity and mechanisms of resistance in comparison to a *XIAP* deletion.

TNF receptor-associated factor 3 (TRAF3)
Tumor necrosis factor receptor associated factors (TRAFs) are crucial intracellular signaling molecules, responsible for conveying signals initiated by the RLR- (RIG-I-Like receptor), TNFR-, TLR- (Toll-Like receptor) and IL-1R- (interleukin-1 receptor) families. TRAFs mediate the link between receptor activation and the assembly of signaling complexes, ultimately leading to activation of downstream effectors. TRAFs also have a role as E3-ligases, enabling the formation of polyubiquitin chains on signaling molecules (Häcker *et al.,* 2011). *TRAF3* is located on chromosome 14 (UniProt, Q13114).

As mentioned above, TRAF3 acts as a negative regulator of the non-canonical NF-κB pathway by regulating NIK turnover together with TRAF2, cIAP1 and cIAP2 (Liao *et al.,* 2004; Zarnegar *et al.,* 2008). Deletion of *TRAF3* results in constitutive NFKB2/p100 processing into p52 and thus activation of the non-canonical NF-κB pathway (Keats *et al.,* 2007). Moreover, homozygous deletion of *TRAF3* is enriched in relapse patients (Chavan *et al.,* 2017). Its possible role in drug resistance, however, remains unclear.

CYLD
CYLD is a deubiquitinating enzyme located on chromosome 16 which can deconjugate ubiquitin chains from proteins (UniProt Q9NQC7; Sun, 2010). CYLD is a negative regulator of both the non-canonical and canonical NF-κB pathway by deubiquitinating several key molecules of these pathways, thereby silencing the signal (Brummelkamp *et al.,* 2004; Kovalenko *et al.,* 2003; Trompouki *et al.,* 2003; McDaniel *et al.,* 2016).

Loss of *CYLD* results in a higher NF-κB signature expression and also protects cells against TNF-α induced apoptosis (Annunziata *et al.,* 2007; Brummelkamp *et al.,* 2004). Chromosome 16q deletion can be correlated with worse overall survival, likely due to the loss of *CYLD* (Jenner *et al.,* 2007; Walker *et al.,* 2010; van Andel 2016). Low CYLD expression is correlated with poor overall progression free survival with abolished Wnt-signaling most likely to be the cause (van Andel *et al.,* 2016). Its possible role in resistance to therapy remains to be elucidated.

Current treatment in MM
Many forms of therapy exist to combat MM. These therapies include, among others, chemotherapy, pharmalocigal therapy with for instance proteasome inhibitors such as bortezomib, stem cell transplantation and treatment with immunomodulatory drugs (IMiDs) (Barlogie *et al.,* 2004; Annunziata *et al.,* 2007; Keats *et al.,* 2007; Krönke *et al.,* 2014). IMiD treatment combined with dexamethasone is often used in patients. One such IMiD is pomalidomide. Pomalidomide is classified as a third-generation IMiD, and is a thalidomide analogue. It is more potent than its family members thalidomide or lenalidomide (Quach *et al.,* 2009). Lenalidomide is widely prescribed to newly-diagnosed patients, whilst pomalidomide is often only utilized in relapsed/refractory setting (Holstein *et al.,* 2017). Dexamethasone is a corticosteroid often used in conjunction with other forms of therapy (Sinha *et al.,* 2010; Siegel *et al.,* 2019). Pomalidomide in combination with dexamethasone has been shown to be effective for patients who become lenalidomide-resistant (Siegel et al., 2019). What effect *BIRC2, BIRC3, CYLD* or *TRAF3* deletions have on pomalidomide and dexamethasone sensitivity remains unknown.

Deletions of BIRC2, BIRC3, TRAF3 and CYLD in MM

This study aims to further understand the role of *BIRC2*, *BIRC3*, *TRAF3* and *CYLD* deletions in relapse and possible drug resistance. Using CRISPR/Cas9 knock out (KO) cells, we investigated the effects of these deletions on resistance to clinical drugs pomalidomide and dexamethasone. In addition, we examined the differential expression of targets of clinical drugs and various NF-κB markers. Examining the effect of a *BIRC2*, *BIRC3*, *CYLD* or *TRAF3* deletion in comparison to a *XIAP* deletion will be interesting with regard to drug sensitivity and possible methods of resistance.

Materials and methods

Generation of sgRNA plasmids

To generate sgRNA plasmids for the KO of *BIRC2, BIRC3*, *CYLD* and *TRAF3*, sgRNAs were designed with the help of the CrisPick tool (Doench *et al.,* 2016; Sanson *et al.,* 2018). From this, the predicted top 4 best sgRNAs were chosen (Appendix A, Table S1). Using these sequences, oligos containing a BsmbI restriction site overhang were ordered from Integrated DNA Technologies. pLKO5.sgRNA.hU6.GFP , pLKO5.hU6.sgRNA.dTom and pLKO5.hU6.sgRNA.PURO, kindly gifted by the Dana–Farber Cancer Institute Harvard Medical School, were used for sgRNA cloning. Forward and reverse sgRNA oligos were annealed using PCR, and diluted 1:500 in nuclease-free water. Vectors were digested using BmsBI. sgRNAs were subsequently subcloned into the BsmBI restriction enzyme site using T4-ligase. All constructs were verified by sequencing. *BIRC2*, *TRAF3* and *CYLD* sgRNAs were cloned into the pLKO5.hU6.sgRNA.dTom vector. *BIRC3* sgRNAs were cloned into the pLKO5.sgRNA.hU6.GFP vector. *XIAP* sgRNAs were cloned into the pLKO5.sgRNA.hU6.PURO vector

Lentiviral generation

HEK293T cells were seeded in 2 mL at a density of 0.75x10^6 cells per well in a 6-well plate and supplemented with DMEM (Thermo Fisher Scientific, Waltham, USA) containing 10% FCS and 1% Penicillin-Streptomycin. Cells were maintained for 24 hours at 37 °C with 5% CO_2 in humidified atmosphere. 1000 ng of psPAX2 (No. 12260, Addgene) and 200 ng pMD2.G (No. 12259, Addgene) were mixed with 1000 ng of vector of interest. Vectors of interest included the following: the pLKO5d.SSF.SpCas9.P2a.BSD vector (No. 57821, Addgene) for Cas9 expression; sgRNA vectors made as described above for generation of KOs; Luciferase or POLR2A vectors for control; pLKO5.sgRNA.hU6.GFP or pLKO5.sgRNA.hU6.dTom vectors without any sgRNA for the generation of fluorescent cells in competition assays. 250 µL of Opti-MEM I Reduced Serum Medium (Thermo Fisher Scientific, Waltham, USA) was added to the DNA mixture. 6 µL Trans-LT1 (Mirus Bio LLC, Madison, WI) was added and incubated at 23 °C for 0.5 hours. After incubation, the mixture was added dropwise onto cells. After 6 hours, medium was changed to DMEM (Thermo Fisher Scientific, Waltham, USA) containing 30% FCS and 1% Penicillin-Streptomycin. After 96 hours, medium with virus was harvested and sterilized using a 0.45 µm pore size filter. Virus was frozen at -80 °C until use.

Transduction of cell lines

For the generation of CRISPR/Cas9 KO cells, cell lines MM.1S, OPM2 and JJN3 were used. These cell lines were obtained from ATCC (Manassas, Virginia, USA) and the German Collection of Microorganisms and Cell Cultures GmbH (DSMZ, Braunschweig, Germany). Cells were maintained in Advanced RPMI 1640 Medium (Thermo Fisher Scientific, Waltham, USA) supplemented with 10% fetal bovine serum (FCS), 1% Penicillin-Streptomycin and 1% L-glutamine. For transduction of cell lines, $1x10^6$ cells were seeded in a 48-well plate in 500 µL medium. Next, 200 µL of Cas9 virus medium was added to cells, and cells were spun at 1200 rpm for 1 hour at 32 °C. Cells were then maintained at 37 °C with 5% CO_2 in a 100% humidified atmosphere. After 72 hours, blasticidin selection was performed using 5 µg/mL (InvivoGen, San Diego, USA). Cells were kept under selection for 72 hours. After 7 days of recovery, cells were transduced with sgRNA vectors. Cells transduced with XIAP sgRNA vector were selected using 2 µg/mL puromycin for 72 hours (InvivoGen, San Diego, USA). Cells transduced with Luciferase, *BIRC2*, *BIRC3*, *CYLD* or *TRAF3* sgRNA vectors, were analyzed using fluorescence-activated cell sorting (FACS). For competition assays, fluorescent cells were made by transducing cells with pLKO5.sgRNA.EFS.GFP or pLKO5.sgRNA.EFS.dTom virus in a likewise manner. Cells were then analyzed using FACS.

FACS analysis

The percentage of transduced cells was determined by using the sgRNA vector-derived fluorescence. Cells were washed 2 times in 1X phosphate-buffered saline (PBS) and resuspended in PBS. Samples were then FACSed using a CytoFLEX Flow Cytometer (Beckman Coulter Life Sciences). Samples were analyzed using the FlowJo™ v10.8 Software (BD Life Sciences). Competition assays were analyzed in a likewise manner.

Western Blot Analysis

To prepare cells for Western Blot, cells were washed 2 times with 1X PBS. Cells were lysed using Pierce Lysis Buffer (Thermo Fisher Scientific, Waltham, USA) with added protease inhibitor (Thermo Fisher Scientific, Waltham, USA) for 15 minutes. Cell lysate was cleared by centrifugation for 10 min at 12000 rpm at 4 °C. Protein concentration was measured using a Pierce™ BCA Protein Assay Kit (Thermo Fisher Scientific, Waltham, USA) according to the manufacturer's instructions. Protein concentration was normalized and 10-20 µg of protein was loaded per sample. Samples were denatured and separated by sodium dodecyl sulfate-polyacrylamide gel electrophoresis (SDS-PAGE). Proteins were transferred to an Immobilon-P polyvinylidene difluoride membrane (Millipore, Bedford, MA). Membranes were blocked with 5% milk in TBST (tris-buffered saline/Tween20) for 1 hour. Membranes were washed in TBST 3 times for 10 minutes. Primary antibodies were diluted in 5% BSA in TBST. Incubation was performed overnight at 4 °C. Membranes were washed in TBST 3 times for 10 minutes. Secondary antibody was diluted in 5% milk in TBST and membranes were incubated for 1 hour at room temperature. Protein detection was performed using Pierce™ ECL Western Blotting-Substrate (Thermo Fisher Scientific, Waltham, USA) according to the manufacturer's instructions. Membranes were imaged with the ChemiDoc XRS + System (Bio-Rad, Munich, Germany). After imaging, membranes were incubated for 10 minutes in Restore™ Western Blot Stripping Buffer (Thermo Fisher Scientific, Waltham, USA). After brief reactivation with methanol, membranes were blocked with 5% milk in TBST for one hour. Membranes were washed with TBST, and membranes were then used for further probing. Antibodies used from Cell signaling (Danvers, USA) include:
IKZF1 (clone D6N9Y, #14859, 1:1000), IKZF3 (clone D1C1E, #15103, 1:1000)

c-IAP2 (clone 58C7, #3130, 1:1000), TRAF3 (#4729, 1:1000), XIAP (clone D228W, #14334, 1:1000), CYLD (clone D1A10, #8462, 1:1000), NF-κB p65 (clone D14E12, #8242T, 1:1000), Phospho-NF-κB p65 (clone 93H1, #3033, 1:1000), NF-κB2 p100/p52 (#4882S, 1:1000), anti-rabbit IgG HRP-linked antibody (#7074, 1:5000), anti-mouse IgG HRP-linked antibody (#7076, 1:5000). Antibodies used from Bio-Rad (Mississauga, ON, Canada) include: c-IAP1 (clone AB01/3B4, #VMA00532, 1:1000). Antibodies used from Sigma-Aldrich (St. Louis, USA) include anti-α-Tubulin (#T5168, 1:7000). Equal protein loading was confirmed by detection of tubulin.

Cell viability assay
Cells were seeded in a 96-well plate with respective treatments. Plates were incubated at 37 °C with 5% CO_2 in humidified atmosphere for 96 hours. Next, cells were treated with CellTiter-Glo®Luminescent Cell Viability Assay (Promega, Madison, USA) according to manufacturer's instructions. Luminescence was detected using the POLARStar Omega plate reader (BMG LabTech, Ortenberg, Germany). Conditions were normalized to the dimethyl sulfoxide- (DMSO) (Sigma Aldrich, Taufkirchen, Germany) treated controls.

Competition assay
Cells were seeded in a 6-well plate with respective treatments. KO cells and fluorescent cells cells were seeded in a 3/7 ratio respectively. Cells were maintained in Advanced RPMI 1640 Medium (Thermo Fisher Scientific, Waltham, USA) supplemented with 10% fetal bovine serum (FCS), 1% Penicillin-Streptomycin and 1% L-glutamine. Medium with respective treatments was changed every 3 days. For FACS analysis, cells were washed in 1X PBS 2 times, and analyzed as described above.

Transient Knock Down (KD) of cIAP1
For the transient KD of cIAP1 chemical compound Gü3394, kindly provided by the University of Bonn, was used. This compound induces cIAP1 auto-degradation. Cell lines used for this experiment included MM.1S, JJN3, AMO1, NCI-H929, RPMI-8226 and U266. These cell lines were obtained from ATCC (Manassas, Virginia, USA) and the German Collection of Microorganisms and Cell Cultures GmbH (DSMZ, Braunschweig, Germany). The compound was added to cells at a concentration of 0.1 µM and cells were maintained in Advanced RPMI 1640 Medium (Thermo Fisher Scientific, Waltham, USA) supplemented with 10% fetal bovine serum (FCS), 1% Penicillin-Streptomycin and 1% L-glutamine. Every 3 days medium supplemented with compound or respective DMSO control was refreshed. After 2 weeks of treatment, cells were either maintained in the presence of Gü3394/DMSO or were put off treatment completely. Cells were then maintained for 2 weeks before analyzing via Real-time quantitative PCR (RT-qPCR). For cell viability assays, cells were kept under Gü3394 or DMSO pressure for a week. After a week the respective cell viabilities were set up as described above, whilst still adding Gü3394 or DMSO on top of drug treatment.

qPCR analysis
Total RNA for all samples was isolated using the RNeasy Mini Kit (Qiagen, Hilden, Germany) according to manufacturer's instructions. RNA was transcribed into complementary DNA (cDNA) using TaqMan Reverse Transcription Reagents (ThermoFisher Scientific, Waltham, USA) according to the manufacturer's instructions. RT-qPCR was performed using the StepOneTM Real-Time PCR (Applied Biosystems, USA). SYBR Green Master Mix (Thermo Fisher Scientific, Waltham, USA) was used. Thermal cycling conditions were as follows: 95 °C for 5 min, followed by 45 cycles of 95 °C for

10 seconds and 60 °C for 30 seconds. Expression fold change was calculated using the $2^{-(\Delta\Delta Ct)}$ method as described by Livak and Schmittgen (2001). Primer pair sequences used are as follows: 5′-CAATGACCCCTTCATTGACC-3′ and 5′-GACAAGCTTCCCGTTCTCAG-3′ for *GAPDH*; 5'- CCCCTGTAAGCGATACTCCA-3' and 5'- TGGGAGCCATTCATTTTCTC-3' for *IKZF1*; 5'- GGACACTGACAGCAACCATG-3' and 5'- CATCACCTCCCCTTCCTTGT-3' for *IKZF3*; 5'- ATGTGGAGATCATTGAGCAGC-3' and 5'- CCTGGTCCTGTGTAGCCATT-3' for *RelA*; 5'- CTGGAGCAAGAGGCCAAAGA-3' and 5'-ACAGAGCCTGCTGTCTTGTC-3' for *NFKB2*.

Statistical analysis
Graphs were constructed using GraphPad PRISM for Mac version 8.0.0 (GraphPad Software, San Diego, USA). Statistical differences were evaluated using GraphPad Prism. Statistical significance was set at $p<0.05$ (*), $p<0.01$(**), $p<0.001$(***) and $p<0.0001$ (****). $P \geq 0.05$ was considered to be non-significant (n.s.).

Results

cIAP1, cIAP2, XIAP, CYLD and TRAF3 are differentially expressed across MM cell lines

To determine endogenous protein expression levels, cell lines MM.1S, OPM2 and JJN3 were tested for protein expression levels of cIAP1, cIAP2, XIAP, CYLD and TRAF3 via Western Blot (fig. 1A). CYLD expression was comparable across all cell lines. Differential expression of cIAP1, cIAP2, XIAP and TRAF3 was seen across the different cell lines (fig. 1A-B). Remarkably, expression of cIAP2 was not detectable in OPM2 cells, whereas it was expressed moderately in MM.1S cells and highest expression was seen in JJN3. Similarly, no TRAF3 protein expression was detected in MM.1S while in OPM2 TRAF3 was expressed moderately, and in JJN3, expression was highest. This expression profiling allowed for comparison of the effect of protein knock out under differing endogenous protein levels. Cell lines were also probed for NF-κB markers p65 and p-p65, and IKZF1 (Ikaros) and IKZF3 (Aiolos), which are essential transcription factors in MM (Krönke *et al.,* 2014). Differing expression levels of the NF-κB markers and essential transcription factors could be observed across cell lines.
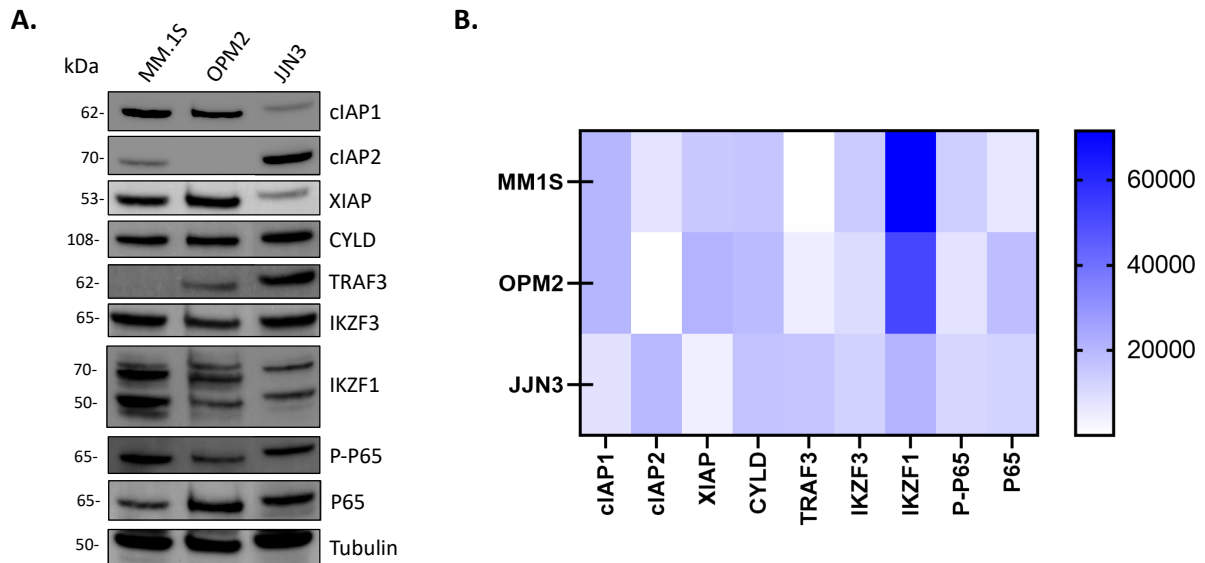
Figure 1: Expression levels of cIAP1, cIAP2, XIAP, CYLD, TRAF3 and various NF-κB markers and crucial transcription factors across different MM cell lines. *(A) Western Blot of proteins of interest for cell lines MM.1S, OPM2 and JJN3. (B) Heatmap representing raw gray values of Western Blot. Gray values were corrected for differential loading using tubulin.*

## Generation of KO cells using the CRISPR/Cas9 system

To ensure transduction of cells with the sgRNA vector was successful, cells were analyzed using FACS and Western Blot. Different sgRNA vectors for each KO were tested (Appendix B, fig. 1-3). Transduction efficiency was analyzed using FACS, whilst the ability of the sgRNA to knock out *BIRC2*, *BIRC3*, *XIAP*, *CYLD* or *TRAF3* was confirmed through Western Blot. 2-4 sgRNAs were tested per KO. From this, the best performing sgRNAs were chosen and used for further experiments (Appendix B, fig. 1-3; fig. 2). *BIRC2*-targeting sgRNA is as follows: 5'- CATGGGTAGAACATGCCAAG-3'. *BIRC3*-targeting sgRNA is as follows: 5'- CATGGGTTCAACATGCCAAG – 3'. *XIAP*-targeting sgRNA is as follows: 5'- TCTGACCAGGCACGATCACA- 3'. *CYLD*-targeting sgRNA is as follows: 5'- TCACTGACGGGGTGTACCAA- 3'. *TRAF3*-targeting sgRNA is as follows: 5'- GCCCGAAGCAGACCGAGTGT- 3'. For MM.1S transduction efficiency lay at 87.2-94.6% (fig. 2G) Transduction efficiency in JJN3 was 86.7-99.1% (fig. 2H). Transduction efficiency of OPM2 lay at 76.1-96.5% (fig. 2I). The exact way of gating can be found in appendix B, figure 1-3. KO of all targets in all cell lines was successful, as shown in figure 2A-F.
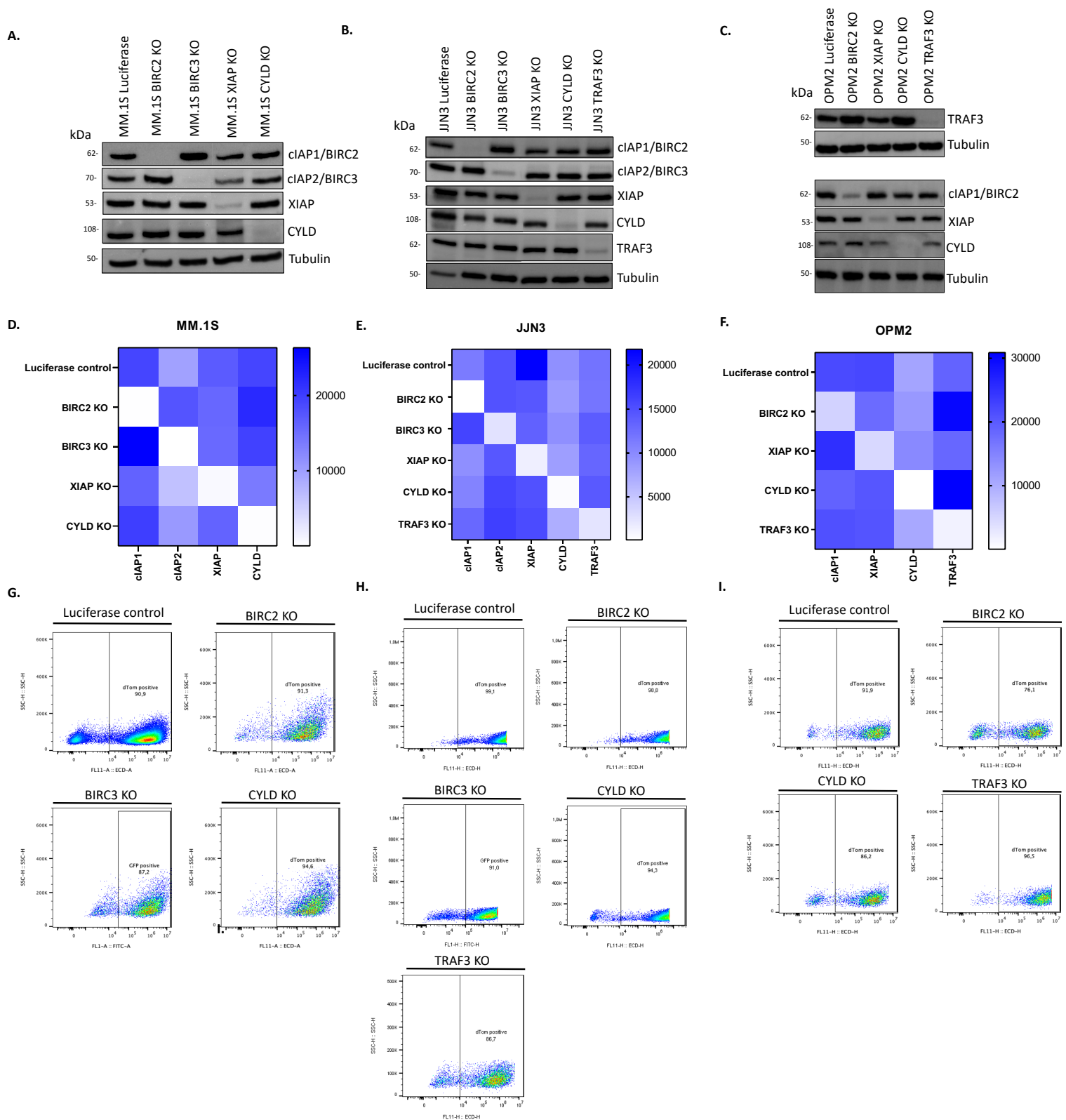
Figure 2: Transduction of MM.1S, JJN3 and OPM2. *(A) Western Blot of MM.1S Luciferase control, BIRC2 KO, BIRC3 KO, XIAP KO and CYLD KO. (B) Western Blot of JJN3 Luciferase control, BIRC2 KO, BIRC3 KO, XIAP KO, CYLD KO and TRAF3 KO. (C) Two Western Blots of OPM2 Luciferase control, BIRC2 KO, XIAP KO, CYLD KO and TRAF3 KO. Loading of both blots is in the same order. (D-F) Heatmap representing raw gray values of Western Blot MM.1S, JJN3 and OPM2. Values are corrected for differential loading using Tubulin. (G) FACS analysis of MM.1S Luciferase and KO cells. (H) FACS analysis of JJN3 Luciferase and KO cells. (I) FACS analysis of OPM2 Luciferase and KO cells*

13

BIRC2, BIRC3, XIAP, CYLD and TRAF3 KO confer resistance to pomalidomide and dexamethasone

To investigate whether deletion of *BIRC2*, *BIRC3*, *XIAP*, *CYLD* or *TRAF3* could be responsible for increased drug resistance, MM.1S and OPM2 cell lines were treated with dexamethasone and pomalidomide at various concentrations. Since IMiDs in combination with dexamethasone are an integral part of patient treatment, we investigated the contribution of *BIRC2*, *BIRC3*, *XIAP*, *CYLD* or *TRAF3* deletion to resistance to this form of therapy in MM.1S, OPM2 and JJN3 cell lines. KO cell lines of MM.1S and OPM2 were subjected to 1 and 5 µM of dexamethasone or pomalidomide for 96 hours, after which cell viability was assessed. In MM.1S cells, increased cell viability after dexamethasone treatment at both 1 and 5 µM was observed when *BIRC2*, *BIRC3*, *XIAP* and *CYLD* knock-out was effectuated (fig. 3A). *BIRC3* KO resulted in the highest difference compared to control, followed by *BIRC2*, *CYLD* and *XIAP* respectively. In OPM2 a similar trend could be observed (fig. 3A). *BIRC2*, *XIAP*, *CYLD* and *TRAF3* deletion all led to increased resistance to dexamethasone at both 1 and 5 µM (fig. 3A). KO cells also became more resistant to pomalidomide treatment at both 1 and 5 µM in both MM.1S and OPM2 (fig. 3B). Resistance to dexamethasone and pomalidomide individually therefore seems independent of the cell line used, and can be attributed solely to *BIRC2*, *BIRC3*, *XIAP*, *CYLD* and *TRAF3* deletion. Since treatment with pomalidomide and dexamethasone is often used in conjunction, cell lines were also treated with a combination of pomalidomide and dexamethasone, both at 5 µM (fig. 3C). Deletion of *BIRC2* and *CYLD* led to increased resistance to combinatorial treatment, with statistical significance reach in two out of the three cell lines. Deletion of *BIRC3* and *TRAF3* in cell lines expressing these proteins led to increased resistance to combinatorial treatment as well. In MM.1S, *XIAP* deletion led to increased sensitivity to combinatory treatment, whilst in OPM2 it led to increased resistance. In JJN3, *BIRC2*, *XIAP* and *CYLD* deletion did not lead to a significant increase in resistance, although a similar trend comparable to MM.1S could be observed here (fig. 3C). So whilst the effects of *XIAP* deletion in combinatory treatment seem to be cell line specific, deletions of *BIRC2*, *BIRC3*, *CYLD* and *TRAF3* confer resistance to combinatory treatment across different cell lines.
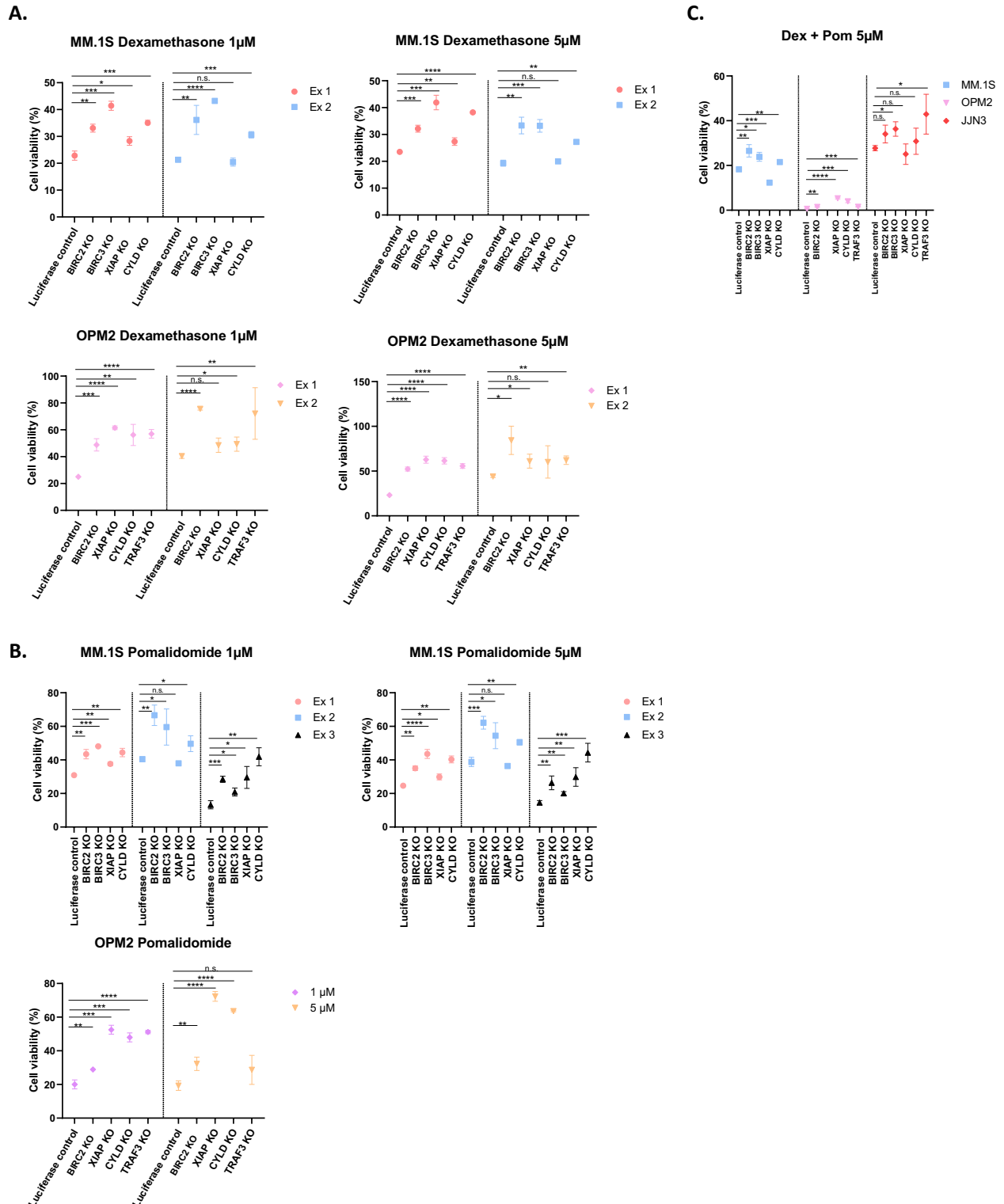
Figure 3: Cell viability assay of KO cell lines treated with pomalidomide and dexamethasone. *(A) Cell viability of MM.1S and OPM2 KO cell lines after 96 hours of dexamethasone treatment at 1 or 5 µM (N=3 technically independent replicates). Cell viability is normalized to respective DMSO conditions. Data represents the mean ± SD. Experiments were repeated twice, indicated by the dashed separation line. (B) Cell viability assay of MM.1S and OPM2 KO cell lines after 96 hours of pomalidomide treatment at 1 or 5 µM (N=3 technically independent replicates). Cell viability is normalized to respective DMSO conditions. Data represents the mean ± SD. Experiments for MM.1S cell lines were repeated three times, indicated by the dashed separation line. Experiments for OPM2 cell line are shown at 1 and 5 µM separated by the dashed separation line. (C) Cell viability of MM.1S, OPM2 and JJN3 KO cell lines after 96 hours of dexamethasone and pomalidomide combinatory treatment at 5 µM (N=3 technically independent replicates). Cell viability is normalized to respective DMSO conditions. Data represents the mean ± SD.*

15

Population doubling of BIRC2, BIRC3 and CYLD KO cells is comparable to control

To assess whether *BIRC2*, *BIRC3* or *CYLD* KO gave cells a proliferative advantage over their luciferase control, MM.1S KO and control cells were seeded in a 6-well plate at 2.5 x 10^5 cells/mL. Cell count was then tracked manually for 15 days. No noticeable difference could be observed in the proliferation curve of KO cells compared to the control (fig. 4A). Therefore, it can be concluded there is no proliferative advantage when *BIRC2*, *BIRC3* or *CYLD* is deleted under normal conditions.

BIRC2, BIRC3, XIAP, CYLD or TRAF3 deletions confer proliferative advantage under therapeutic pressure of pomalidomide and dexamethasone

As shown above, deletion of *BIRC2*, *BIRC3*, *XIAP*, *CYLD* and *TRAF3* resulted in an increased resistance to both pomalidomide and dexamethasone treatment. The next question addressed was if deletion of these genes would lead to a proliferative advantage over cells without these deletions, specifically under treatment conditions. To investigate whether KO of *BIRC2*, *BIRC3*, *XIAP*, *CYLD* or *TRAF3* led to a proliferative advantage under pomalidomide or dexamethasone treatment conditions, a competition assay using either dTomato or GFP fluorescent MM.1S or OPM2 cells seeded together with the KO cell lines was set up. Cells were treated with 0.01 µM pomalidomide or 0.001 µM dexamethasone for 14 days and the percentage of green and red fluorescent cells was tracked and analyzed using FACS (Appendix B, fig. S5-S13). To show that the KO cells did not already have a proliferative advantage over these cells under control conditions, the percentage of cells with the KO when under DMSO conditions was tracked during 14 days without treatment. As shown in figure 4B, no significant change in the percentage of cells could be observed, indicating that these cells did not have a proliferative advantage over the fluorescent cells under control conditions. MM.1S *BIRC2*, *BIRC3*, *XIAP* and *CYLD* KO were all able to outgrow the cells without these deletions when undergoing treatment (fig. 4C). Taken together with the DMSO control, this means that these deletions only give cells an advantage when under treatment conditions, and not when treatment is absent. To investigate whether this finding was cell line specific, a similar competition assay was set up for the OPM2 KO cell lines. However, possibly due to undergoing lentiviral transduction twice, these cells were more sensitive to treatment compared to the fluorescent control cells they were seeded with. When compared to the luciferase control (which was also transduced twice) however, a similar trend could be observed as with the MM.1S cell line. For treatment with both pomalidomide and dexamethasone, *BIRC2*, *XIAP*, *CYLD* and *TRAF3* KO were all able to resist treatment longer than the luciferase control, showing again that these deletions confer a proliferative advantage during treatment conditions over cells without these deletions (fig. 4D).
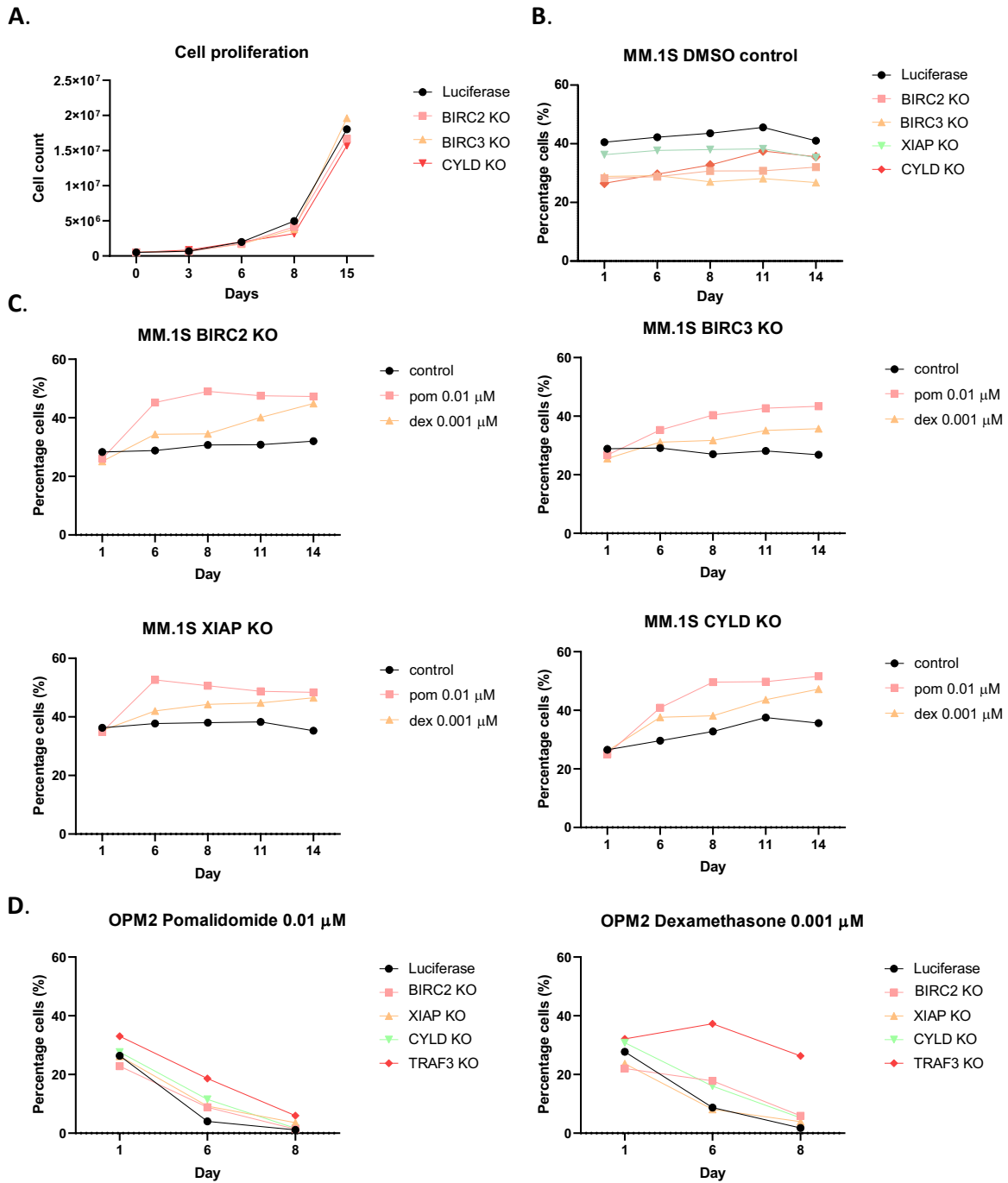
Figure 4: Competition assay of MM.1S and OPM2 KO cell lines over 8 to 14 days. *(A) Cell proliferation of various MM.1S KO cells over 15 days. Cells were counted manually as cells/mL and total cell number was then calculated. BIRC2, BIRC3 and CYLD KO are depicted in pink, orange and red respectively. Luciferase control is depicted in black. (B) DMSO control of MM.1S luciferase control and KO cell lines over 14 days. Percentage of cells means percentage of KO cell lines as measured by FACS (Appendix B, fig. S4-S8). Cells were seeded together with MM.1S cells without deletion. (C) MM.1S BIRC2, BIRC3, XIAP and CYLD KO under 0.1 μM pomalidomide or 0.001 μM dexamethasone treatment during 14 days. Control cell line is KO cell line treated with DMSO. Cells were seeded together with MM.1S cells without deletion. Percentage of cells means percentage of KO cell lines as measured by FACS (Appendix B, fig. S4-S8) (D) Percentage of OPM2 KO cell lines under 0.1 μM pomalidomide or 0.001 μM dexamethasone treatment during 8 days. Percentage of cells means percentage of KO cell lines as measured with FACS (Appendix B, fig. S9-S13). Cells were seeded together with OPM2 cells without deletion.*

17

BIRC2, BIRC3, XIAP or CYLD KO results in upregulation of IKZF1 protein levels

One main target of pomalidomide is the neosubstrate IKZF1. Upon pomalidomide treatment, this transcription factor is degraded by altering substrate specificity of CRBN to degrade IKZF1 (Krönke *et al.,* 2014). IKZF1 is a transcription factor which plays an important role in B-cell development (Merkenschlager, 2010). Since IKZF1 is a target of pomalidomide treatment, and KO cells were shown to be more resistant to pomalidomide, MM.1S KO cells were evaluated for their IKZF1 protein levels via Western Blot. *BIRC2*, *BIRC3*, *XIAP* and *CYLD* KO cells all showed an increase in IKZF1 protein levels when compared to luciferase control (fig. 5A-B). *CYLD* KO had the most pronounced effect on IKZF1 protein levels, followed by *BIRC2* KO, *BIRC3* KO and finally *XIAP* KO. IKZF1 overexpression has been shown to reduce MM cell sensitivity to lenalidomide (Krönke *et al.,* 2017). It is therefore likely that the increased resistance to pomalidomide seen in the MM.1S KO cell lines is the result of an increase in IKZF1 levels.
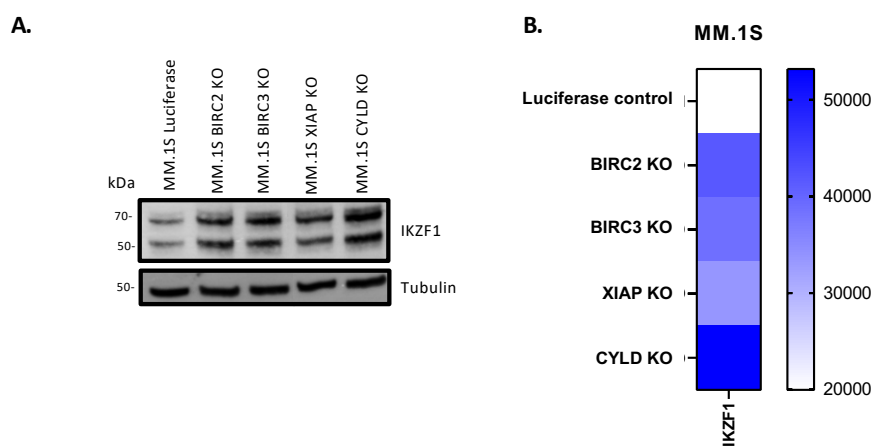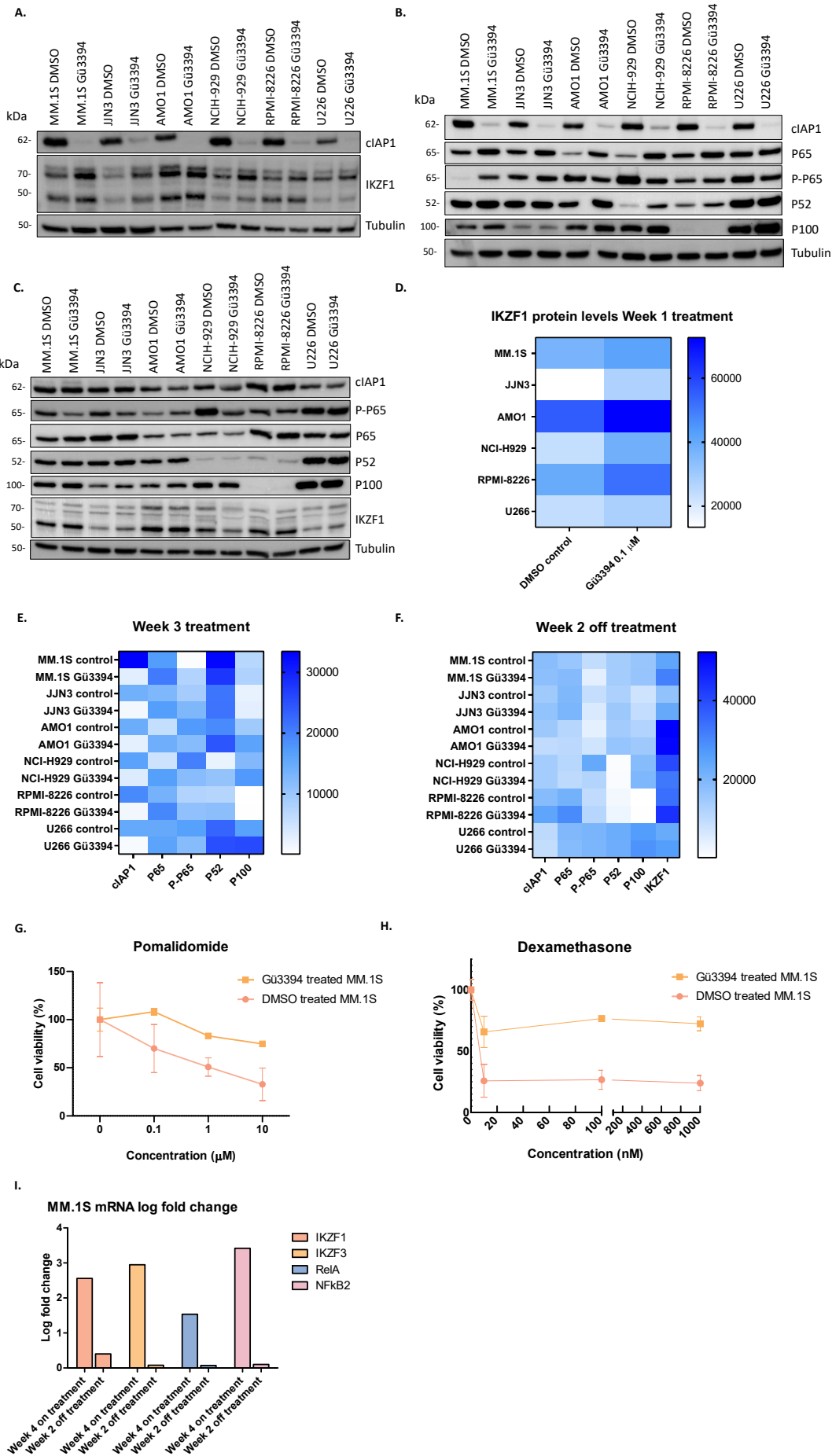

Figure 5: Cell proliferation and IKZF1 protein levels in KO cells. (A) Western Blot of MM.1S Luciferase control, BIRC2 KO, BIRC3 KO, XIAP KO and CYLD KO. (B) Heat map showing raw gray values of blot in fig. 5A. Values are corrected for differential loading using Tubulin.

Transient KD of cIAP1 results in transcriptional changes of IKZF1, IKZF3 and various markers of the NF-κB pathway

To investigate if the upregulation of IKZF1 found in the KO cells was universal across various MM cell lines, and to also evaluate possible upregulation of other transcription factors such as IKZF3 and markers of the NF-κB pathway, cIAP1 was transiently knocked down using the chemical compound Gü3394. This compound induces auto-degradation of cIAP1 and allows for direct manipulation of cIAP1 levels. This also allowed us to see if upregulation of IKZF1 and possibly other proteins was reversible when cIAP1 levels were restored. Gü3394 was added to cells at a concentration of 0.1 μM. This concentration did not have any effect on cell viability (data not shown) whilst still being able to induce cIAP1 degradation (fig. 6 A-B, D-E). Cells were evaluated for IKZF1 levels, and were also tested for various markers of the NF-κB pathway, namely p100, p52, p65 and phosphorylated p65 (p-p65). Protein levels of these cells were compared to their respective DMSO controls. After one week of treatment, IKZF1 levels of MM.1S, JJN3, AMO1, NCI-H929, RPMI-8226 and U266 cell lines were evaluated. All cell lines showed an upregulation of IKZF1 protein levels to at least some degree (fig. 6A, D). Most prominent were the differences in cell lines MM.1S, JJN3 and NCI-H929, where a distinct

upregulation of IKZF1 could be observed. After 3 weeks on treatment, cells were also evaluated for p65, p-p65, p100 and -52 levels. P65 was upregulated in all cell lines (fig. 6B, E). However, phosphorylation of p65 (p-p65) was only slightly upregulated in MM.1S, JJN3, and RPMI-8226, whilst in AMO1, NCI-H929 and U266 p-p65 was slightly downregulated (fig. 6B, E). P100 was upregulated in all cell lines, and with that upregulation could also be seen of its cleaved version p52 (fig. 6B, E). We examined if this upregulation was reversible by keeping cells under Gü3394 or DMSO treatment for two weeks, and then took cells off treatment and maintained them for another two weeks. cIAP1 levels returned to normal, and cells were evaluated again for their IKZF1, p65, p-p65, p100 and p52 levels (fig. 6C, F). In all cell lines, levels of p65, p-p65, p100 and p52 returned to normal after cIAP1 auto-degradation was stopped. Differences in IKZF1 levels also returned to normal in most cell lines, with only slight differences in some cell lines. This shows that there is a direct correlation between the upregulation of markers of the NF-κB pathway and IKZF1 and the presence or absence of cIAP1. To confirm Gü3394-treated cells were also more resistant to dexamethasone and pomalidomide, comparable to the KO of cIAP1, cells were treated with a range of concentrations of respective drugs in the presence of Gü3394. Gü3394-treated cells were more resistant to both dexamethasone and pomalidomide, again highlighting the correlation between cIAP1 absence and increased resistance to treatment (fig. 6G, H). We next examined if upregulation of IKZF1, IKZF3, p100 and p65 was transcriptional or post-transcriptional, a qPCR was performed comparing Gü3394 to DMSO treated MM.1S cells. Cells were either on treatment for four weeks, or on treatment for two weeks and then taken off of treatment for two weeks before qPCR was performed. mRNA levels of IKZF1, IKZF3, p100 (RelA) and p65 (NFkB2) were tested. When treated for 4 weeks with Gü3394, there was an upregulation of IKZF1-, IKZF3-, p100- and p65- mRNA levels when compared to DMSO control (fig. 6I). When comparing that to the 2 weeks on - 2 weeks off treatment samples, it is also shown that this transcriptional upregulation is reversible, and can therefore directly be linked to the absence of cIAP1. The RT-qPCR should be repeated to make sure data is reproducible.

A.

kDa			
62-			cIAP1
70- / 50-			IKZF1
50-			Tubulin

B.

kDa		
62-		cIAP1
65-		P65
65-		P-P65
52-		P52
100-		P100
50-		Tubulin

C.

kDa		
62-		cIAP1
65-		P-P65
65-		P65
52-		P52
100-		P100
70- / 50-		IKZF1
50-		Tubulin

D.

IKZF1 protein levels Week 1 treatment

E.

Week 3 treatment

F.

Week 2 off treatment

G.

Pomalidomide

H.

Dexamethasone

I.

MM.1S mRNA log fold change

20

Figure 6: Chemical KD of cIAP1. *(A) Western Blot of chemical KD of cIAP1 with Gü3394. Cells were put on Western Blot after 1 week of treatment. (B) Western blot of chemical KD of cIAP1 with Gü3394 after 3 weeks of treatment. (C) Western blot of chemical KD of cIAP1 with Gü3394 after 2 weeks on treatment, and then 2 weeks off treatment completely. (D)Heatmap of raw gray values of Western blot fig. 6A. Values are corrected for differential loading using Tubulin. (E) Heatmap of raw gray values of Western blot fig. 6B. Values are corrected for differential loading using Tubulin. (F) Heatmap of raw gray values of Western blot fig. 6B. Values are corrected for differential loading using Tubulin. (G) Cell viability assay of DMSO or Gü3394 treated cells treated with various concentrations of pomalidomide (N=3 technically independent replicates). Cell viability is normalized to respective DMSO conditions. Data represents the mean ± SD. (H) Cell viability assay of DMSO or Gü3394 treated cells treated with various concentrations of dexamethasone (N=3 technically independent replicates). Cell viability is normalized to respective DMSO conditions. Data represents the mean ± SD (I) mRNA levels of IKZF1, IKZF3, RelA(p65) and NFKB2 (p100) in MM.1S cells upon treatment of 0.1 µM Gü3394 for 4 week, or 2 weeks on treatment and then 2 weeks off treatment (N=1 biologically independent replicate). mRNA expression is normalized to GAPDH levels and DMSO conditions.*

Discussion

BIRC2, *BIRC3*, *CYLD* and *TRAF3* deletions are genetic mutations that are specifically enriched in relapse patients and loss of these genes is associated with poor prognosis and worse overall progression free survival in MM patients. The exact role they play in possible resistance to therapy was however unclear. The aim of this study was to elucidate the possible role of these deletions in resistance to therapy and relapse of disease.

We show that cIAP1, cIAP2, CYLD and TRAF3 proteins are expressed differentially among different MM cell lines. For instance, cIAP2 is not expressed in OPM2 and TRAF3 is not expressed in MM.1S. Endogenous levels of these proteins differ per cell line.

Using CRISPR/Cas9 mediated knock-out, we found that *BIRC2*, *BIRC3*, *CYLD* and *TRAF3* deletions are associated to pomalidomide and dexamethasone resistance in MM cell lines MM.1S and OPM2. Interestingly, *XIAP* deletion, which hitherto has not been associated to relapse or poor progression free survival in MM, but is a protein involved in the same pathways, was also able to induce pomalidomide and dexamethasone resistance. This indicates that resistance to these forms of therapy may not only be associated to these genes specifically, but rather is a consequence of deletions or mutations of any gene associated with a similar role in the NF-κB pathway and/or apoptotic pathway. In combinatory treatment however, the effect of *XIAP* deletion seemed to be cell line specific, which perhaps is why deletion of *XIAP* is not seen significantly in relapse patients.

To see if deletion of *BIRC2*, *BIRC3* or *CYLD* gave a proliferative advantage to cells, we tracked the cell count of cells carrying these deletions over the course of 15 days. We found that carrying any of these deletions did not give cells a proliferative advantage over control cells. We also found that under DMSO control conditions, deletion of *BIRC2, BIRC3, XIAP* and *CYLD* did not have a significant effect on cell proliferation. Importantly however, when treated with dexamethasone and/or pomalidomide the cells harboring these deletions outgrew control cells without these deletions. This suggests that *BIRC2*, *BIRC3* and *CYLD* deletions are not driver mutations in the sense that they give cells a growth advantage over other cells under normal conditions. Under pressure of treatment however, these deletions do create a growth advantage as was shown in the competition assays. This also would explain why deletions in these genes are usually not significantly found at diagnosis, but rather are selected at relapse or refractory MM.

We investigated whether resistance of these deletion-bearing cells to pomalidomide could be explained by looking at a known target of pomalidomide, namely IKZF1. KO cells were evaluated for IKZF1 protein levels via Western Blot and compared to their control cell line. Although the exact mechanism remains unclear, we show that IKZF1 protein levels are elevated when *BIRC2*, *BIRC3*, *XIAP* or *CYLD* is knocked out. Since IKZF1 overexpression has been shown to reduce MM cell sensitivity to lenalidomide (Krönke *et al.,* 2017), it is

conceivable that the increment of IKZF1 protein levels is one of the main causes of the resistance of these KO cells to pomalidomide. How *BIRC2*, *BIRC3*, *XIAP*, *CYLD* and *TRAF3* deletions cause dexamethasone resistance remains to be investigated.

To investigate whether IKZF1 protein level increase was universal across different MM cell lines, and to also evaluate other transcription factors and markers of the NF-κB pathway across multiple cell lines, we made use of the compound Gü3394, which induces auto-degradation of cIAP1. Cells were treated with Gü3394 or control DMSO, and maintained for a week. Cells were then evaluated for their IKZF1 protein levels via Western Blot. We showed that upon cIAP1 degradation, IKZF1 protein levels were elevated in all MM cell lines tested. When cells were subsequently taken off Gü3394-pressure, cIAP1 levels returned to normal, and consequently IKZF1 protein levels returned to normal as well. This shows that this phenomenon is reversible and can be directly linked to the presence or absence of cIAP1, as also shown in the KO cells. Upon cIAP1 degradation, MM.1S cells also became more resistant to both pomalidomide and dexamethasone treatment again, further confirming our results with the KO cell lines.

The cell lines MM.1S, JJN3, AMO1, NCI-H929, RPMI-8226 and U266 were also tested for various NF-κB markers p65, p-p65, p100 and p52 when treated with Gü3394. Upon cIAP1 degradation, p65 levels were elevated in all cell lines. Its phosphorylated version, p-p65 was only upregulated in MM.1S, JJN3 and RPMI-8226. In AMO1, NCI-H929 and U266 a slight downregulation of p-p65 could be observed. P100 was shown to be upregulated upon cIAP1 degradation in all cell lines, and its cleaved version p52 followed this trend as well. When cells were put off Gü3394-pressure, and cIAP1 levels returned to normal, so did protein levels of p65, p-p65, p100 and p52. This shows that this upregulation of NF-κB markers is reversible, in a similar fashion as also seen with IKZF1. Since activation of the NF-κB pathway is thought to contribute to relapse mechanisms in MM, upregulation of p65, p-p65, 100 and p52 when cIAP1 is absent strongly suggests cIAP1-deletion to be a driver in forming resistance (Magrangeas *et al.,* 2013).

To see if upregulation of these factors had a transcriptional or post-transcriptional origin, RT-qPCR was performed on DMSO- or Gü3394-treated cells to see if mRNA levels were upregulated. Cells were either on treatment for four weeks, or on treatment for two weeks and then off of treatment for two weeks before qPCR was performed. mRNA levels of *IKZF1*, *IKZF3*, *RelA* (p65) and *NFKB2* (p100) were tested. Upon cIAP1 degradation, mRNA levels of all these factors increased, and this upregulation could be reversed when Gü3394 treatment was stopped. This indicates that elevated protein levels of IKZF1, IKZF3, p65 and p100 have their roots in a transcriptional upregulation. How specifically this transcriptional upregulation of *IKZF1* and *IKZF3* is regulated, remains to be investigated.

Mutations in the NF-κB pathway may lead to increased resistance to certain forms of therapy, but potentially could also create increased sensitivity to other forms of therapy, which, if true, could be exploited clinically. One way to investigate this would be through a CRISPR/Cas9 synthetic lethality screen. Comparing a MM cell line without any of these deletions to the same cell line in which one of these genes is knocked out, would allow to find vulnerabilities in the KO cells which could translate to targets for therapy aiming to specifically target cells containing deletions of these genes. This could be extremely beneficial for patients harboring these deletions, possibly finding new targets and therefore new forms of therapy.

In conclusion, we show that deletions of *BIRC2*, *BIRC3*, *CYLD* and *TRAF3* result in increased resistance to pomalidomide and dexamethasone, and that this may not be solely a gene-specific phenomenon, but could be a result of alteration of proteins involved in the NF-κB pathway in general. This insight may help to design future therapeutic strategies to overcome resistance in this still incurable disease, with for instance the help of a CRISPR/Cas9 synthetic lethality screen.

Conclusion

In this study we show that *BIRC2*, *BIRC3*, *CYLD* and *TRAF3* deletions, genetic alterations known to be associated to relapse, poor prognosis and worse overall progression free survival, induce pomalidomide and dexamethasone resistance, both to each drug individually and also when combined. *XIAP*-deletion, which is not known to be associated to relapse so far, was also able to induce resistance to these forms of therapy, suggesting a possible commonality in the effect of deletions of genes known to be involved in the NF-κB pathway. Without treatment, deletions in *BIRC2*, *BIRC3* or *CYLD* did not cause a proliferative advantage over control cells. KO cells however did show a proliferative advantage when under pomalidomide or dexamethasone treatment. Pomalidomide resistance could possibly be explained by an upregulation of IKZF1. As shown in the transient KD of cIAP1 with Gü3394, this upregulation of IKZF1 and also IKZF3, another target of pomalidomide, has a transcriptional origin. How *BIRC2*, *BIRC3*, *XIAP*, *CYLD* and *TRAF3* deletions cause dexamethasone resistance remains to be investigated. Transient KD of cIAP1 with Gü3394 also showed upregulation of various NF-κB markers, indicating an activation of the NF-κB pathway when cIAP1 is depleted. The upregulation of p65 and p100 was also shown to have a transcriptional origin. *BIRC2*, *BIRC3*, *CYLD* and *TRAF3* deletions are shown to be drivers of resistance to therapy. It is very interesting to further investigate possible sensitivity of cells harboring these deletions to other forms of therapy, for instance with the help of a CRISPR/Cas9 synthetic lethality screen. This is particularly important, as it could point to forms of therapy for patients with resistant relapse or refractory disease.

Acknowledgements

Literature:

Annunziata CM, Davis RE, Demchenko Y, Bellamy W, Gabrea A, Zhan F, Lenz G, Hanamura I, Wright G, Xiao W, Dave S, Hurt EM, Tan B, Zhao H, Stephens O, Santra M, Williams DR, Dang L, Barlogie B, Shaughnessy JD Jr, Kuehl WM, Staudt LM. Frequent engagement of the classical and alternative NF-kappaB pathways by diverse genetic abnormalities in multiple myeloma. Cancer Cell. 2007 Aug;12(2):115-30. doi: 10.1016/j.ccr.2007.07.004. PMID: 17692804; PMCID: PMC2730509.

Barlogie B, Shaughnessy J, Tricot G, Jacobson J, Zangari M, Anaissie E, Walker R, Crowley J. Treatment of multiple myeloma. Blood. 2004 Jan 1;103(1):20-32. doi: 10.1182/blood-2003-04-1045. Epub 2003 Sep 11. PMID: 12969978.

Bohl SR, Schmalbrock LK, Bauhuf I, Meyer T, Dolnik A, Szyska M, Blätte TJ, Knödler S, Röhner L, Miller D, Kull M, Langer C, Döhner H, Letai A, Damm F, Heckl D, Bullinger L, Krönke J. Comprehensive CRISPR-Cas9 screens identify genetic determinants of drug responsiveness in multiple myeloma. Blood Adv. 2021 May 11;5(9):2391-2402. doi: 10.1182/bloodadvances.2020003541. PMID: 33950175; PMCID: PMC8114551.

Brummelkamp TR, Nijman SM, Dirac AM, Bernards R. Loss of the cylindromatosis tumour suppressor inhibits apoptosis by activating NF-kappaB. Nature. 2003 Aug 14;424(6950):797-801. doi: 10.1038/nature01811. PMID: 12917690

Chavan SS, He J, Tytarenko R, Deshpande S, Patel P, Bailey M, Stein CK, Stephens O, Weinhold N, Petty N, Steward D, Rasche L, Bauer M, Ashby C, Peterson E, Ali S, Ross J, Miller VA, Stephens P, Thanendrarajan S, Schinke C, Zangari M, van Rhee F, Barlogie B, Mughal TI, Davies FE, Morgan GJ, Walker BA. Bi-allelic inactivation is more prevalent at relapse in multiple myeloma, identifying RB1 as an independent prognostic marker. Blood Cancer J. 2017 Feb 24;7(2):e535. doi: 10.1038/bcj.2017.12. PMID: 28234347; PMCID: PMC5386330.

Dejardin E. The alternative NF-kappaB pathway from biochemistry to biology: pitfalls and promises for future drug development. Biochem Pharmacol. 2006 Oct 30;72(9):1161-79. doi: 10.1016/j.bcp.2006.08.007. Epub 2006 Sep 12. PMID: 16970925

Demchenko Y.N., Kuehl W.M., (2010). A critical role for the). NFκB pathway in multiple myeloma. Oncorarget. 1:(1)59-68

Desplanques G, Giuliani N, Delsignore R, Rizzoli V, Bataille R, Barillé-Nion S. Impact of XIAP protein levels on the survival of myeloma cells. Haematologica. 2009 Jan;94(1):87-93. doi: 10.3324/haematol.13483. Epub 2008 Nov 10. PMID: 19001278; PMCID: PMC2625405.

Doench, J. G., Fusi, N., Sullender, M., Hegde, M., Vaimberg, E. W., Donovan, K. F., … Root, D. E. (2016). Optimized sgRNA design to maximize activity and minimize off-target effects of CRISPR-Cas9. Nature biotechnology, 34(2), 184-191. doi:10.1038/nbt.3437

Dutta AK, Alberge JB, Sklavenitis-Pistofidis R, Lightbody ED, Getz G, Ghobrial IM. Single-cell profiling of tumour evolution in multiple myeloma - opportunities for precision medicine.

Nat Rev Clin Oncol. 2022 Jan 11. doi: 10.1038/s41571-021-00593-y. Epub ahead of print. PMID: 35017721.

FlowJo™ Software Version 10.8. Becton, Dickinson and Company; 2021.

Galbán S, Duckett CS. XIAP as a ubiquitin ligase in cellular signaling. Cell Death Differ. 2010 Jan;17(1):54-60. doi: 10.1038/cdd.2009.81. PMID: 19590513; PMCID: PMC2957808

Hayden MS, Ghosh S. NF-κB, the first quarter-century: remarkable progress and outstanding questions. Genes Dev. 2012 Feb 1;26(3):203-34. doi: 10.1101/gad.183434.111. PMID: 22302935; PMCID: PMC3278889.

Häcker, H., Tseng, PH. & Karin, M. Expanding TRAF function: TRAF3 as a tri-faced immune regulator. *Nat Rev Immunol* **11,** 457–468 (2011). https://doi.org/10.1038/nri2998

Hinds, M. G., Norton, R. S., Vaux, D. L. & Day, C. L. Solution structure of a baculoviral inhibitor of apoptosis (IAP) repeat. *Nature Struct. Biol.* **6**, 648–651 (1999).

Holstein SA, McCarthy PL. Immunomodulatory Drugs in Multiple Myeloma: Mechanisms of Action and Clinical Experience. Drugs. 2017 Apr;77(5):505-520. doi: 10.1007/s40265-017-0689-1. PMID: 28205024; PMCID: PMC5705939.

Jenner MW, Leone PE, Walker BA, Ross FM, Johnson DC, Gonzalez D, Chiecchio L, Dachs Cabanas E, Dagrada GP, Nightingale M, Protheroe RK, Stockley D, Else M, Dickens NJ, Cross NC, Davies FE, Morgan GJ. Gene mapping and expression analysis of 16q loss of heterozygosity identifies WWOX and CYLD as being important in determining clinical outcome in multiple myeloma. Blood. 2007 Nov 1;110(9):3291-300. doi: 10.1182/blood-2007-02-075069. Epub 2007 Jul 3. PMID: 17609426.

Karin M. Nuclear factor-kappaB in cancer development and progression. Nature. 2006 May 25;441(7092):431-6. doi: 10.1038/nature04870. PMID: 16724054

Keats JJ, Fonseca R, Chesi M, Schop R, Baker A, Chng WJ, Van Wier S, Tiedemann R, Shi CX, Sebag M, Braggio E, Henry T, Zhu YX, Fogle H, Price-Troska T, Ahmann G, Mancini C, Brents LA, Kumar S, Greipp P, Dispenzieri A, Bryant B, Mulligan G, Bruhn L, Barrett M, Valdez R, Trent J, Stewart AK, Carpten J, Bergsagel PL. Promiscuous mutations activate the noncanonical NF-kappaB pathway in multiple myeloma. Cancer Cell. 2007 Aug;12(2):131-44. doi: 10.1016/j.ccr.2007.07.003. PMID: 17692805; PMCID: PMC2083698.

Keats JJ, Chesi M, Egan JB, Garbitt VM, Palmer SE, Braggio E, Van Wier S, Blackburn PR, Baker AS, Dispenzieri A, Kumar S, Rajkumar SV, Carpten JD, Barrett M, Fonseca R, Stewart AK, Bergsagel PL. Clonal competition with alternating dominance in multiple myeloma. Blood. 2012 Aug 2;120(5):1067-76. doi: 10.1182/blood-2012-01-405985. Epub 2012 Apr 12. PMID: 22498740; PMCID: PMC3412330.

Kovalenko A, Chable-Bessia C, Cantarella G, Israël A, Wallach D, Courtois G. The tumour suppressor CYLD negatively regulates NF-kappaB signalling by deubiquitination. Nature. 2003 Aug 14;424(6950):801-5. doi: 10.1038/nature01802. PMID: 12917691.

Kumar SK, Therneau TM, Gertz MA, Lacy MQ, Dispenzieri A, Rajkumar SV, Fonseca R, Witzig TE, Lust JA, Larson DR, Kyle RA, Greipp PR. Clinical course of patients with relapsed multiple myeloma. Mayo Clin Proc. 2004 Jul;79(7):867-74. doi: 10.4065/79.7.867. PMID: 15244382.

Krönke J, Hurst SN, Ebert BL. Lenalidomide induces degradation of IKZF1 and IKZF3. Oncoimmunology. 2014 Jul 3;3(7):e941742. doi: 10.4161/21624011.2014.941742. PMID: 25610725; PMCID: PMC4292522.

Krönke J, Kuchenbauer F, Kull M, Teleanu V, Bullinger L, Bunjes D, Greiner A, Kolmus S, Köpff S, Schreder M, Mügge LO, Straka C, Engelhardt M, Döhner H, Einsele H, Bassermann F, Bargou R, Knop S, Langer C. IKZF1 expression is a prognostic marker in newly diagnosed standard-risk multiple myeloma treated with lenalidomide and intensive chemotherapy: a study of the German Myeloma Study Group (DSMM). Leukemia. 2017 Jun;31(6):1363-1367. doi: 10.1038/leu.2016.384. Epub 2016 Dec 26. PMID: 28017969

Lau R, Pratt MA. The opposing roles of cellular inhibitor of apoptosis proteins in cancer. ISRN Oncol. 2012;2012:928120. doi: 10.5402/2012/928120. Epub 2012 Aug 9. PMID: 22934195; PMCID: PMC3425795.

Liao G, Zhang M, Harhaj EW, Sun SC. Regulation of the NF-kappaB-inducing kinase by tumor necrosis factor receptor-associated factor 3-induced degradation. J Biol Chem. 2004 Jun 18;279(25):26243-50. doi: 10.1074/jbc.M403286200. Epub 2004 Apr 14. PMID: 15084608.

Livak KJ, Schmittgen TD. Analysis of relative gene expression data using real-time quantitative PCR and the 2(-Delta Delta C(T)) Method. Methods. 2001 Dec;25(4):402-8. doi: 10.1006/meth.2001.1262. PMID: 11846609.

Magrangeas F, Avet-Loiseau H, Gouraud W, Lodé L, Decaux O, Godmer P, Garderet L, Voillat L, Facon T, Stoppa AM, Marit G, Hulin C, Casassus P, Tiab M, Voog E, Randriamalala E, Anderson KC, Moreau P, Munshi NC, Minvielle S. Minor clone provides a reservoir for relapse in multiple myeloma. Leukemia. 2013 Feb;27(2):473-81. doi: 10.1038/leu.2012.226. Epub 2012 Aug 9. PMID: 22874878; PMCID: PMC4157227.

McDaniel DK, Eden K, Ringel VM, Allen IC. Emerging Roles for Noncanonical NF-κB Signaling in the Modulation of Inflammatory Bowel Disease Pathobiology. Inflamm Bowel Dis. 2016 Sep;22(9):2265-79. doi: 10.1097/MIB.0000000000000858. PMID: 27508514; PMCID: PMC4992436.

Merkenschlager M. Ikaros in immune receptor signaling, lymphocyte differentiation, and function. FEBS Lett. 2010 Dec 15;584(24):4910-4. doi: 10.1016/j.febslet.2010.09.042. Epub 2010 Oct 2. PMID: 20888815.

Migliazza A, Lombardi L, Rocchi M, Trecca D, Chang CC, Antonacci R, Fracchiolla NS, Ciana P, Maiolo AT, Neri A. Heterogeneous chromosomal aberrations generate 3' truncations of the NFKB2/lyt-10 gene in lymphoid malignancies. Blood. 1994 Dec 1;84(11):3850-60. PMID: 7949142.

Miller A, Asmann Y, Cattaneo L, Braggio E, Keats J, Auclair D, Lonial S; MMRF CoMMpass Network, Russell SJ, Stewart AK. High somatic mutation and neoantigen burden are correlated with decreased progression-free survival in multiple myeloma. Blood Cancer J. 2017 Sep 22;7(9):e612. doi: 10.1038/bcj.2017.94. PMID: 28937974; PMCID: PMC5709757.

Nagel D, Vincendeau M, Eitelhuber AC, Krappmann D. Mechanisms and consequences of constitutive NF-κB activation in B-cell lymphoid malignancies. Oncogene. 2014 Dec 11;33(50):5655-65. doi: 10.1038/onc.2013.565. Epub 2014 Jan 27. PMID: 24469030

Quach H, Ritchie D, Stewart AK, Neeson P, Harrison S, Smyth MJ, Prince HM. Mechanism of action of immunomodulatory drugs (IMiDS) in multiple myeloma. Leukemia. 2010 Jan;24(1):22-32. doi: 10.1038/leu.2009.236. Epub 2009 Nov 12. PMID: 19907437; PMCID: PMC3922408.

Sanson, K. R., Hanna, R. E., Hegde, M., Donovan, K. F., Strand, C., Sullender, M. E., … Doench, J. G. (2018). Optimized libraries for CRISPR-Cas9 genetic screens with multiple modalities. Nature communications, 9(1), 5416. doi:10.1038/s41467-018-07901-8

Shah V, Sherborne AL, Walker BA, Johnson DC, Boyle EM, Ellis S, Begum DB, Proszek PZ, Jones JR, Pawlyn C, Savola S, Jenner MW, Drayson MT, Owen RG, Houlston RS, Cairns DA, Gregory WM, Cook G, Davies FE, Jackson GH, Morgan GJ, Kaiser MF. Prediction of outcome in newly diagnosed myeloma: a meta-analysis of the molecular profiles of 1905 trial patients. Leukemia. 2018 Jan;32(1):102-110. doi: 10.1038/leu.2017.179. Epub 2017 Jun 6. PMID: 28584253; PMCID: PMC5590713.

Silke J, Meier P. Inhibitor of apoptosis (IAP) proteins-modulators of cell death and inflammation. Cold Spring Harb Perspect Biol. 2013 Feb 1;5(2):a008730. doi: 10.1101/cshperspect.a008730. PMID: 23378585; PMCID: PMC3552501.

Sinha S, Rajkumar SV, Lacy MQ, Hayman SR, Buadi FK, Dispenzieri A, Dingli D, Kyle RA, Gertz MA, Kumar S. Impact of dexamethasone responsiveness on long term outcome in patients with newly diagnosed multiple myeloma. Br J Haematol. 2010 Mar;148(6):853-8. doi: 10.1111/j.1365-2141.2009.08023.x. Epub 2009 Dec 3. PMID: 19958361; PMCID: PMC2864312.

Sun, SC. CYLD: a tumor suppressor deubiquitinase regulating NF-κB activation and diverse biological processes. *Cell Death Differ* **17,** 25–34 (2010). https://doi.org/10.1038/cdd.2009.43

Sun SC. Non-canonical NF-κB signaling pathway. Cell Res. 2011 Jan;21(1):71-85. doi: 10.1038/cr.2010.177. Epub 2010 Dec 21. PMID: 21173796; PMCID: PMC3193406.

The UniProt Consortium, UniProt: the universal protein knowledgebase in 2021, *Nucleic Acids Research*, Volume 49, Issue D1, 8 January 2021, Pages D480–D489, https://doi.org/10.1093/nar/gkaa1100

Trompouki E, Hatzivassiliou E, Tsichritzis T, Farmer H, Ashworth A, Mosialos G. CYLD is a deubiquitinating enzyme that negatively regulates NF-kappaB activation by TNFR family members. Nature. 2003 Aug 14;424(6950):793-6. doi: 10.1038/nature01803. PMID: 12917689.

van Andel H, Kocemba KA, de Haan-Kramer A, Mellink CH, Piwowar M, Broijl A, van Duin M, Sonneveld P, Maurice MM, Kersten MJ, Spaargaren M, Pals ST. Loss of CYLD expression unleashes Wnt signaling in multiple myeloma and is associated with aggressive disease. Oncogene. 2017 Apr;36(15):2105-2115. doi: 10.1038/onc.2016.368. Epub 2016 Oct 24. PMID: 27775078.

Varfolomeev E, Goncharov T, Fedorova AV, Dynek JN, Zobel K, Deshayes K, Fairbrother WJ, Vucic D. c-IAP1 and c-IAP2 are critical mediators of tumor necrosis factor alpha (TNFalpha)-induced NF-kappaB activation. J Biol Chem. 2008 Sep 5;283(36):24295-9. doi: 10.1074/jbc.C800128200. Epub 2008 Jul 11. PMID: 18621737; PMCID: PMC3259840.

Walker BA, Leone PE, Chiecchio L, Dickens NJ, Jenner MW, Boyd KD, Johnson DC, Gonzalez D, Dagrada GP, Protheroe RK, Konn ZJ, Stockley DM, Gregory WM, Davies FE, Ross FM, Morgan GJ. A compendium of myeloma-associated chromosomal copy number abnormalities and their prognostic value. Blood. 2010 Oct 14;116(15):e56-65. doi: 10.1182/blood-2010-04-279596. Epub 2010 Jul 8. PMID: 20616218.

Wang CY, Mayo MW, Korneluk RG, Goeddel DV, Baldwin AS Jr. NF-kappaB antiapoptosis: induction of TRAF1 and TRAF2 and c-IAP1 and c-IAP2 to suppress caspase-8 activation. Science. 1998 Sep 11;281(5383):1680-3. doi: 10.1126/science.281.5383.1680. PMID: 9733516.

Xiao G., Harhaj E.W., Sun S., (2001). NF-κB-Inducing Kinase Regulates the Processing of NF-κB2 p100. Mol. Cell. 7(2):401-409
Senftleben U, Cao Y, Xiao G, Greten FR, Krähn G, Bonizzi G, Chen Y, Hu Y, Fong A, Sun SC, Karin M. Activation by IKKalpha of a second, evolutionary conserved, NF-kappa B signaling pathway. Science. 2001 Aug 24;293(5534):1495-9. doi: 10.1126/science.1062677. PMID: 11520989.

Yang Y, Fang S, Jensen JP, Weissman AM, Ashwell JD. Ubiquitin protein ligase activity of IAPs and their degradation in proteasomes in response to apoptotic stimuli. Science. 2000 May 5;288(5467):874-7. doi: 10.1126/science.288.5467.874. PMID: 10797013.

Zarnegar BJ, Wang Y, Mahoney DJ, Dempsey PW, Cheung HH, He J, Shiba T, Yang X, Yeh WC, Mak TW, Korneluk RG, Cheng G. Noncanonical NF-kappaB activation requires coordinated assembly of a regulatory complex of the adaptors cIAP1, cIAP2, TRAF2 and TRAF3 and the kinase NIK. Nat Immunol. 2008 Dec;9(12):1371-8. doi: 10.1038/ni.1676. Epub 2008 Nov 9. PMID: 18997794; PMCID: PMC2676931.

Supplemental

Appendix A: tables

Table S1: sgRNA sequences used for KO of proteins. sgRNA is reported from 5' to 3' end.

Target	sgRNA 5'-3'
BIRC2	1. ATGCTATGTCAGAACACCGG 2. CATGGGTAGAACATGCCAAG
BIRC3	1. TTTCGTTATTCATTGCACAG 2. CATGGGTTCAACATGCCAAG 3. AGGATTAACTAGAACACTAG 4. ACCCGGAAGTAATGAGTGTG
XIAP	1. ATGACAACTAAAGCACCGCA 2. TCTGACCAGGCACGATCACA 3. TATCAGACACCATATACCCG 4. ACCAGAATTTGTAGACTGCG
CYLD	1. TCACTGACGGGGTGTACCAA 2. TGAGACTGAATGGTAAAGAG 3. ATATTCAAGATCGTTCTGTG 4. ATCCAGTCATAATAAACCAA
TRAF3	1. GCCCGAAGCAGACCGAGTGT 2. CAACTCGCTCGAAAAGAAGG 3. CAGCCAAGCAGAGAAACTGA 4. ATTTACACGCCTTCTCCACG

Appendix B: figures
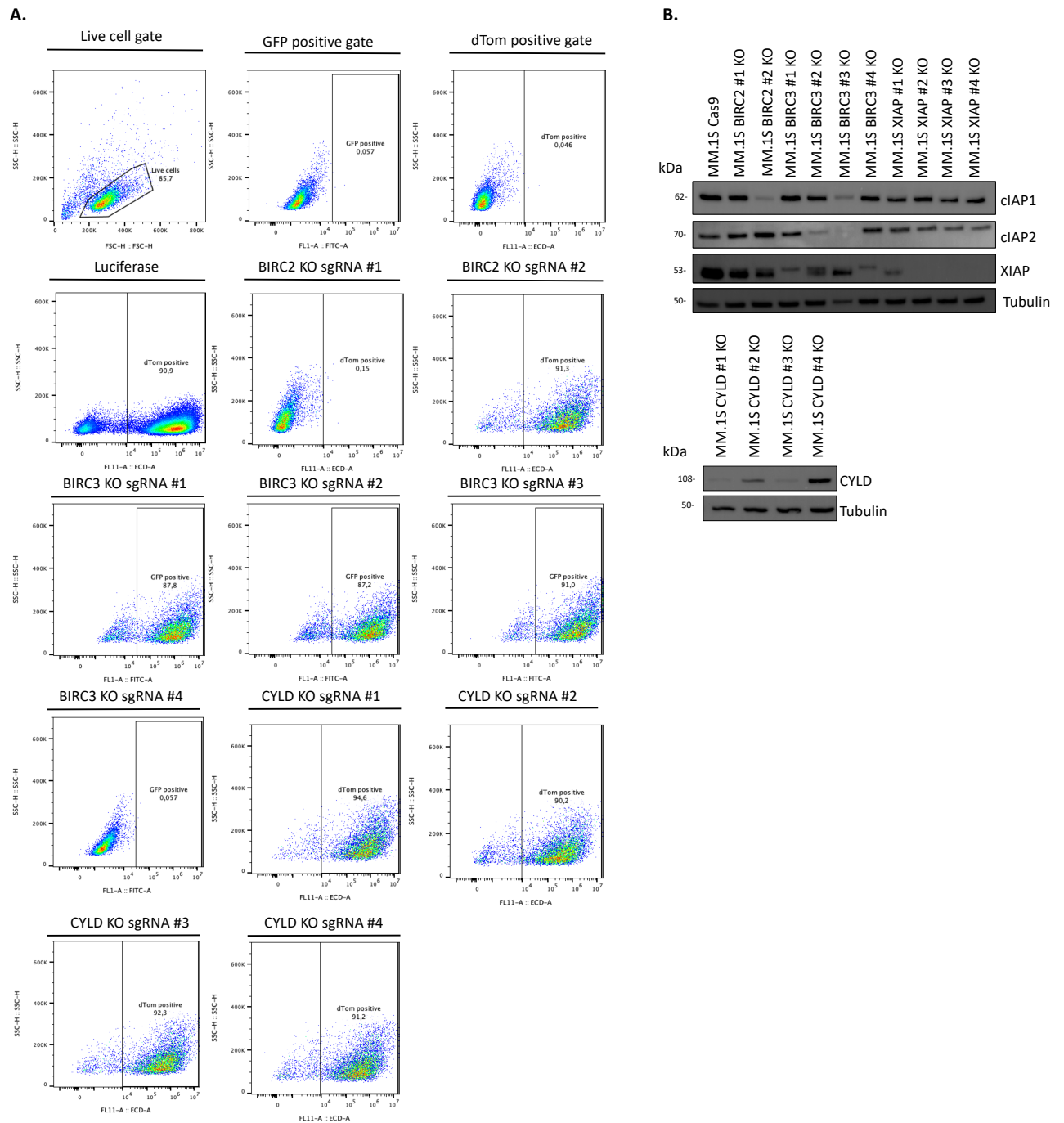
Figure S1: MM.1S FACS and Western Blot analysis of various sgRNAs for BIRC2, BIRC3, XIAP and CYLD. *(A) FACS analysis of various sgRNAs tried for BIRC2, BIRC3 and CYLD KO. Live cell gate, GFP positive gate and dTomato positive gate were decided based based on a MM.1S Cas9 positive cell. Live gate was used for all KO samples prior to dTomato or GFP positive gate. (B) Western Blot analysis of various sgRNAs tried for BIRC2, BIRC3, XIAP and CYLD KO.*
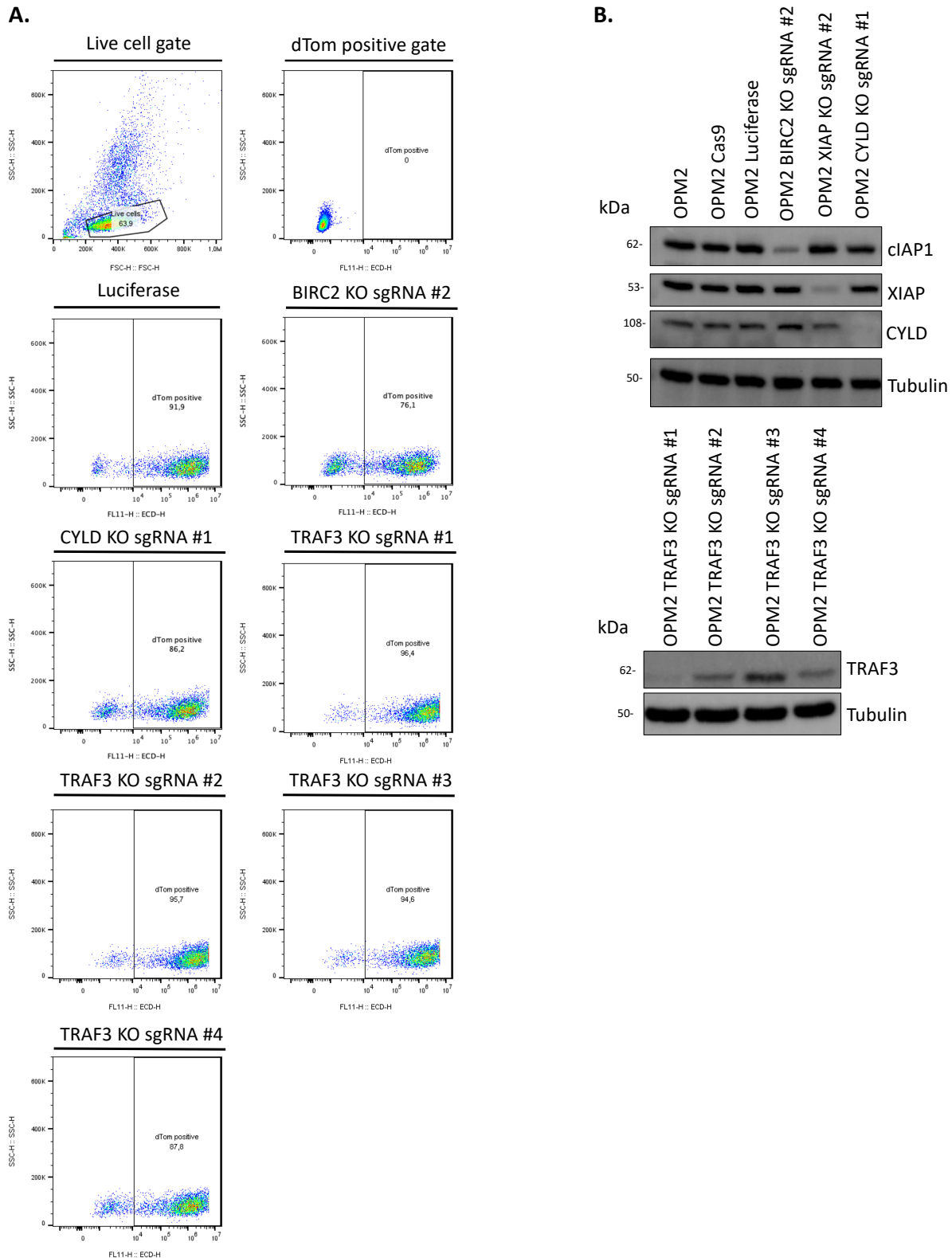
Figure S2: OPM2 FACS and Western Blot analysis of various sgRNAs for BIRC2, XIAP, CYLD and TRAF3. *(A) FACS analysis of various sgRNAs tried for BIRC2, XIAP, CYLD and TRAF3 KO. Live cell gate and dTomato positive gate were decided based based on an OPM2 Cas9 positive cell. Live gate was used for all KO samples prior to dTomato. (B) Western Blot analysis of various sgRNAs tried for BIRC2, XIAP, CYLD and TRAF3.*

31
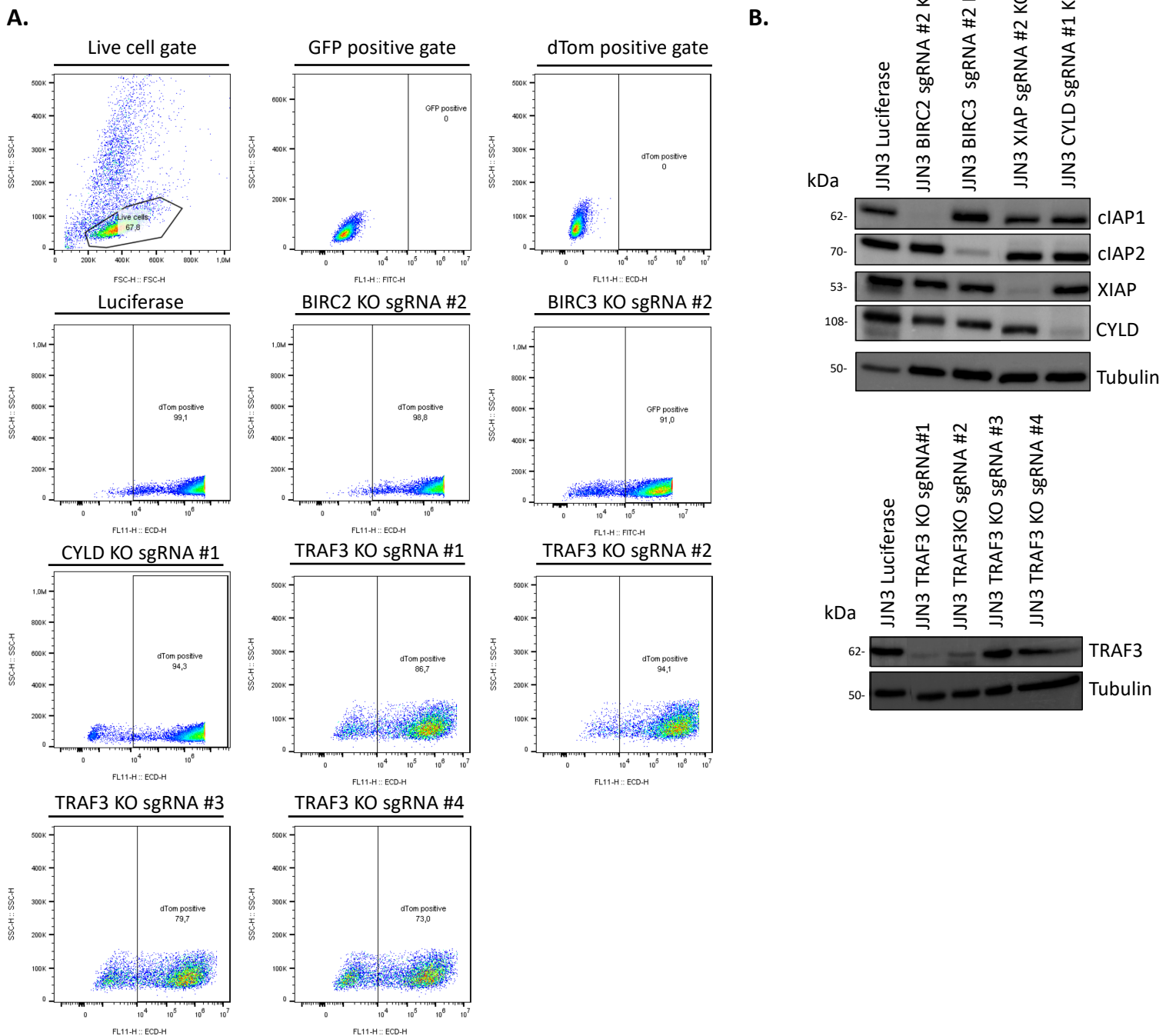
Figure S3: JJN3 FACS and Western Blot analysis of various sgRNAs for BIRC2, BIRC3 XIAP, CYLD and TRAF3. *(A) FACS analysis of various sgRNAs tried for BIRC2, BIRC3, CYLD and TRAF3 KO. Live cell gate, GFP positive gate and dTomato positive gate were decided based based on a JJN3 Cas9 positive cell. Live gate was used for all KO samples prior to dTomato or GFP positive gate. (B) Western Blot analysis of various sgRNAs tried for BIRC2, BIRC3, XIAP, CYLD and TRAF3.*
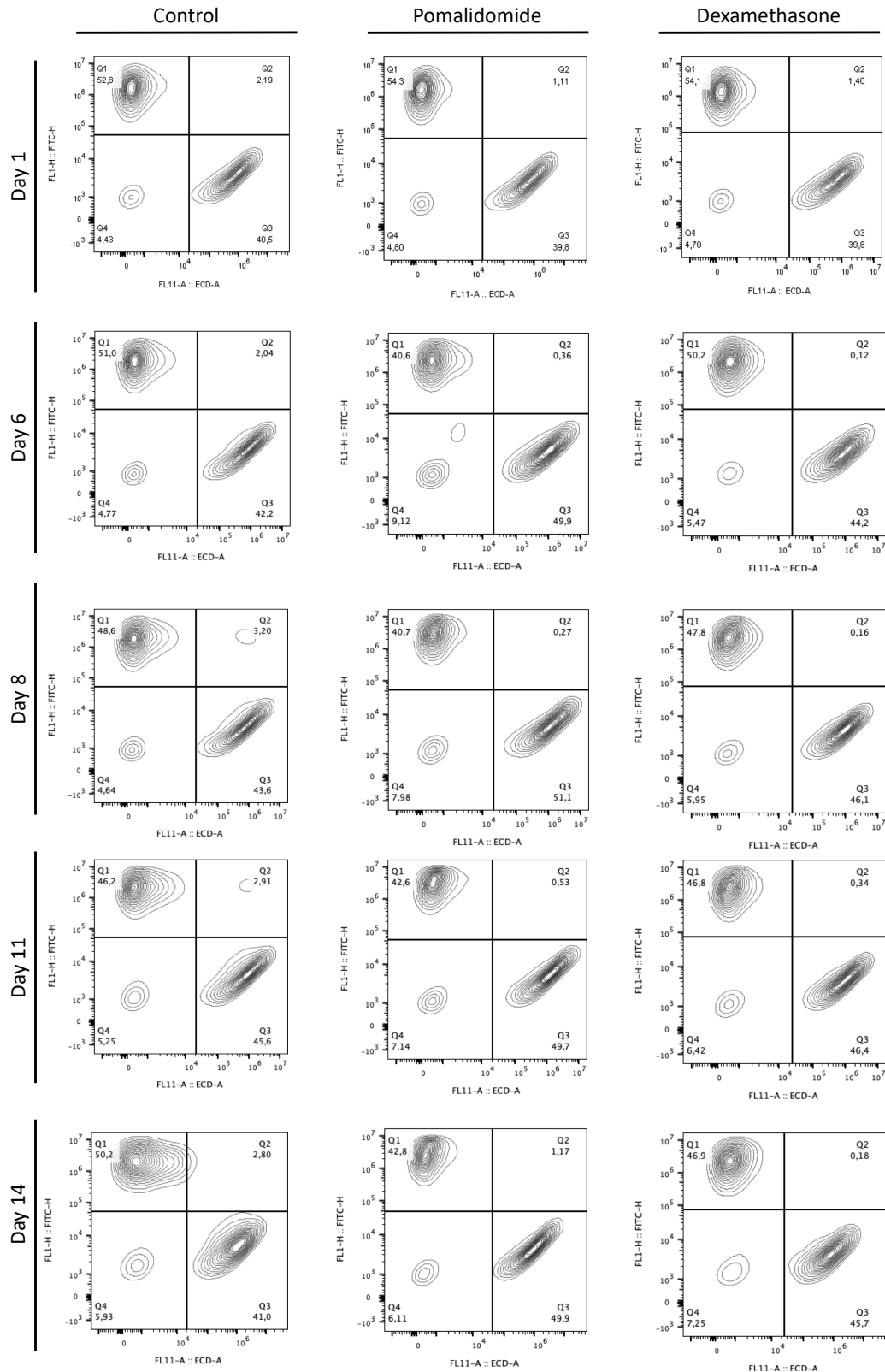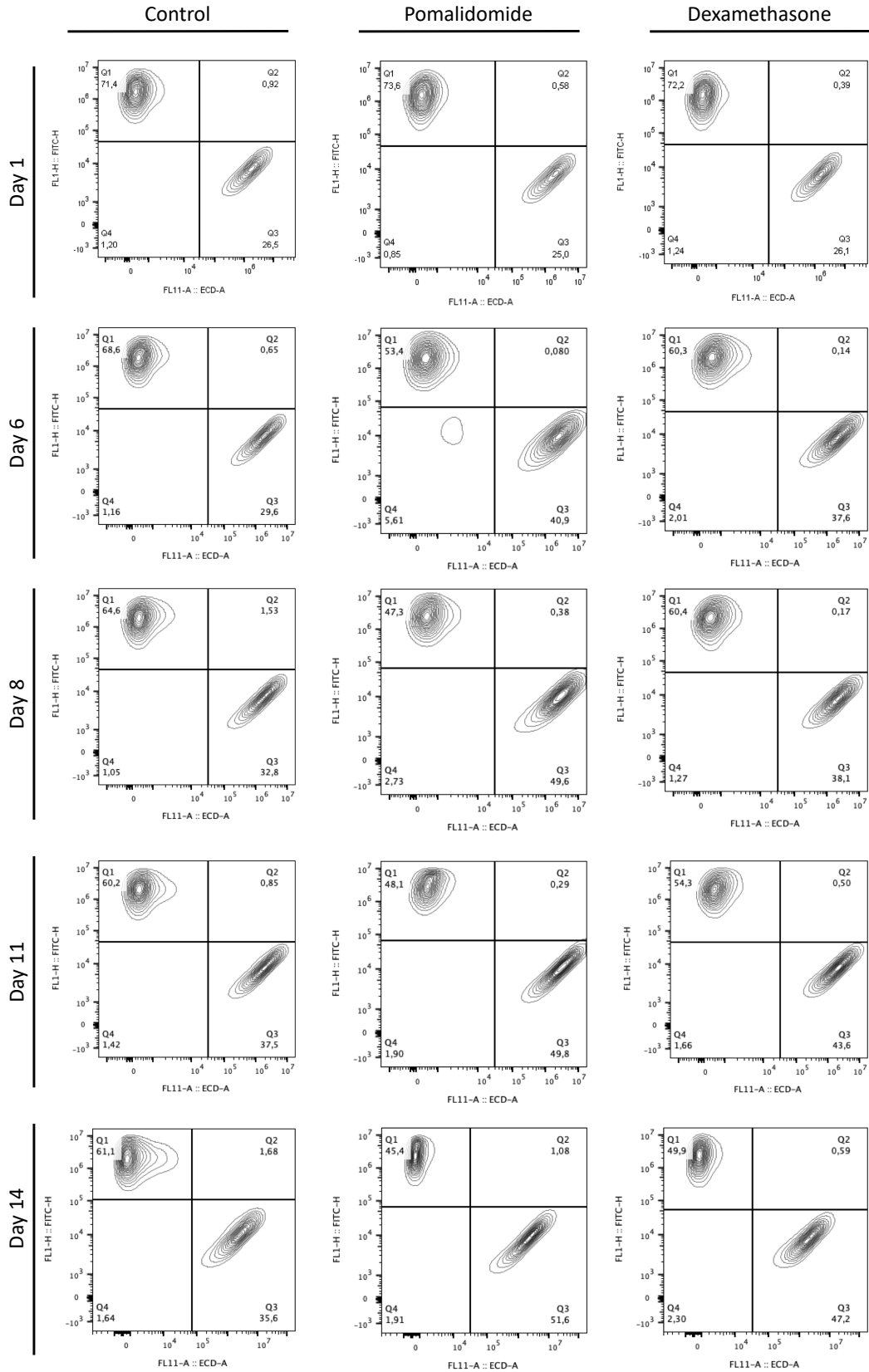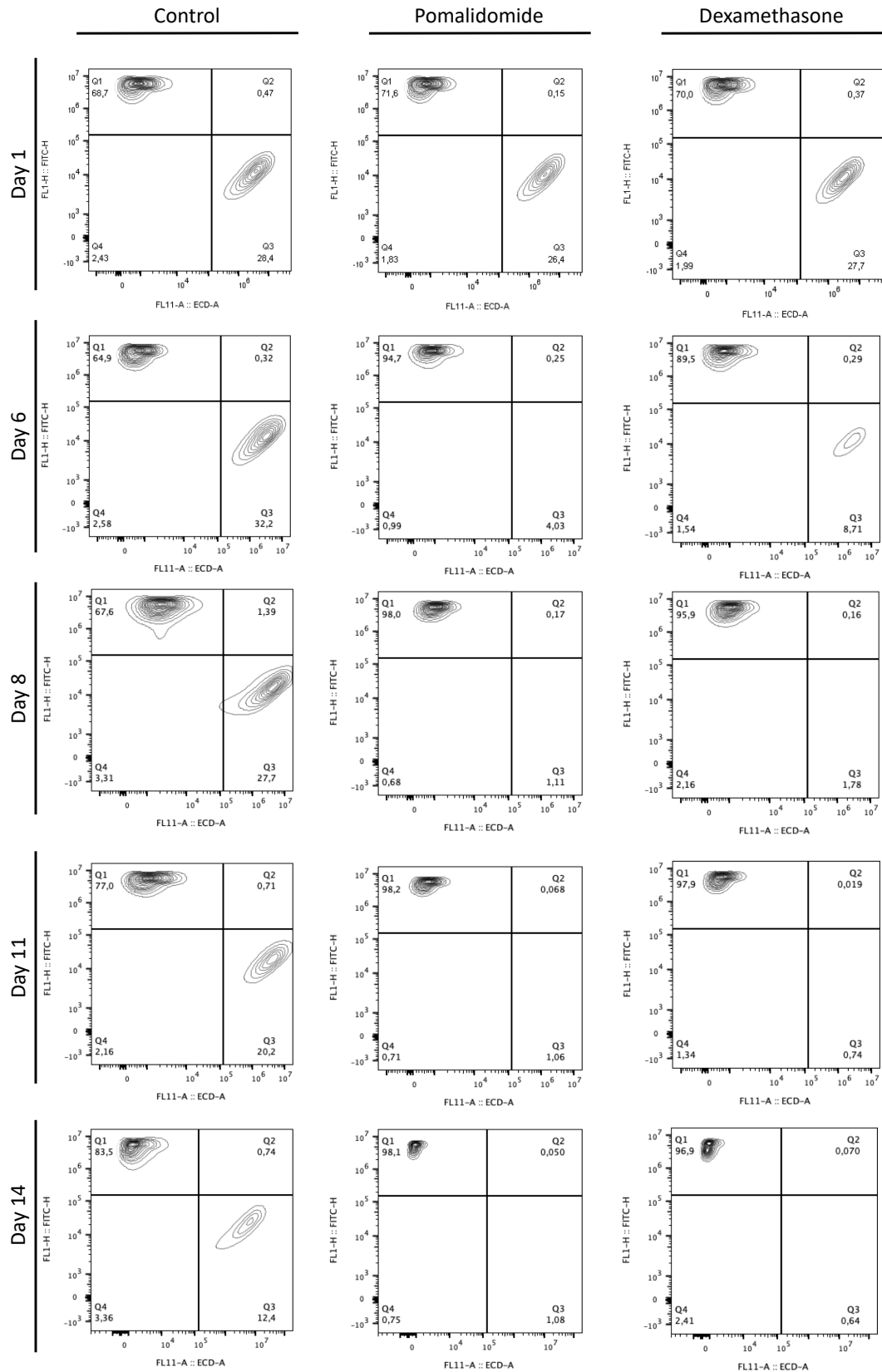
Figure S4: FACS analysis competition assay MM.1S Luciferase. *Cells were gated for live cells prior to FITC-H and ECD-A analysis. Quadrant Q1 was deemed GFP-positive, and quadrant Q3 was deemed dTomato positive. Pomalidomide was added at 0.01 μM. Dexamethasone was added at 0.001 μM over 14 days. Control is DMSO.*
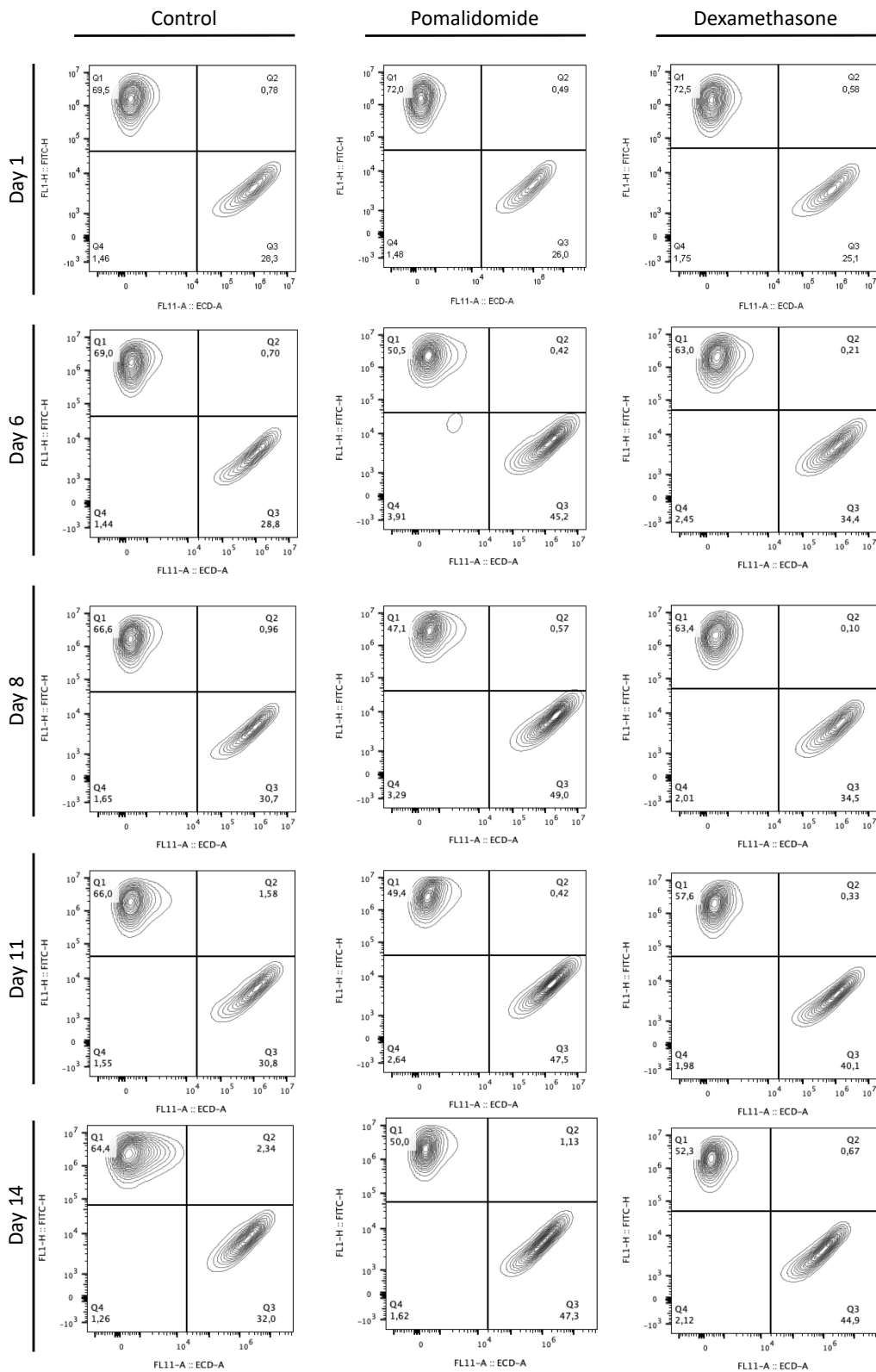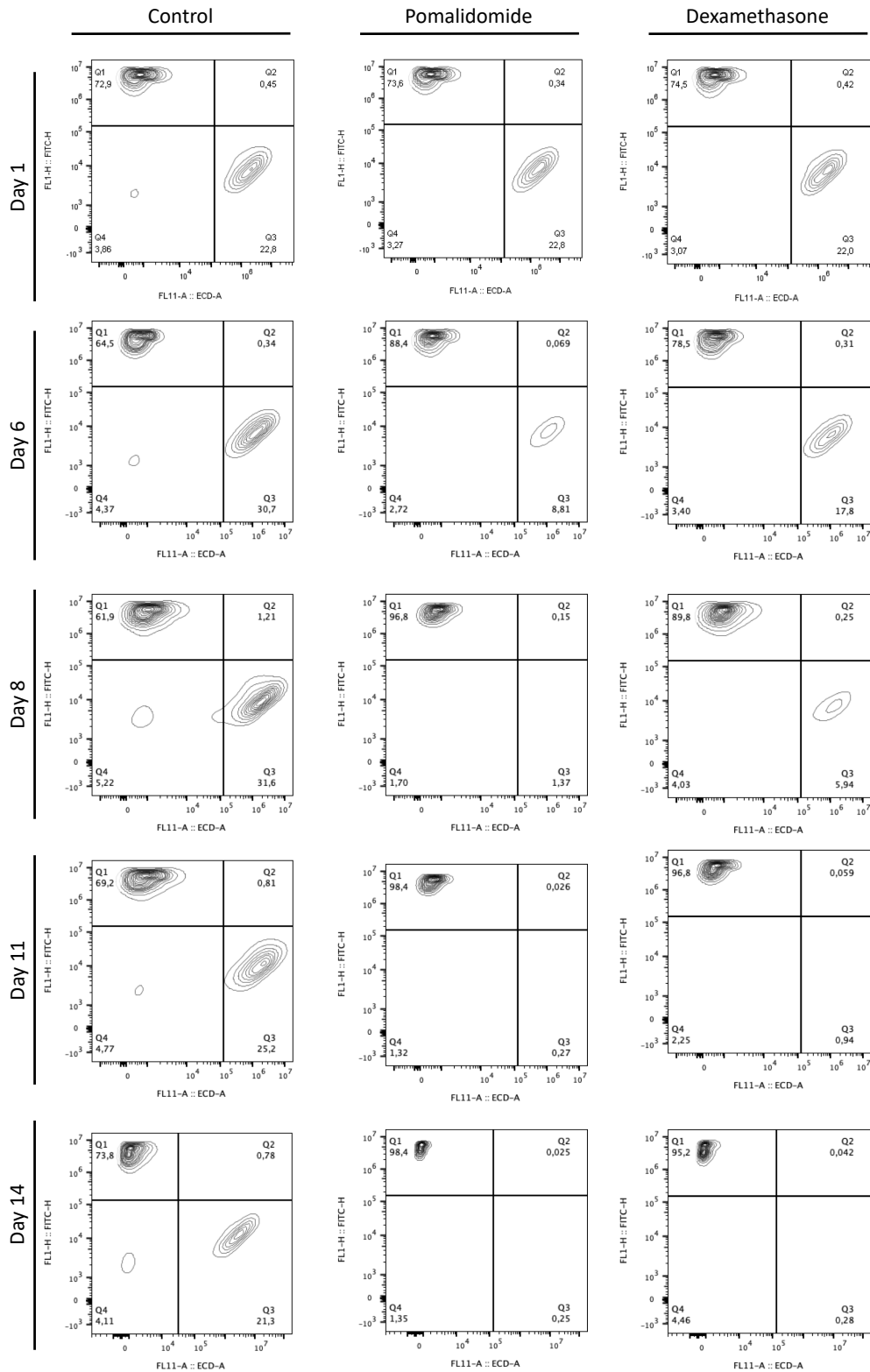
Figure S5: FACS analysis competition assay MM.1S BIRC2 KO. *Cells were gated for live cells prior to FITC-H and ECD-A analysis. Quadrant Q1 was deemed GFP-positive, and quadrant Q3 was deemed dTomato positive. Pomalidomide was added at 0.01 μM. Dexamethasone was added at 0.001 μM over 14 days. Control is DMSO.*
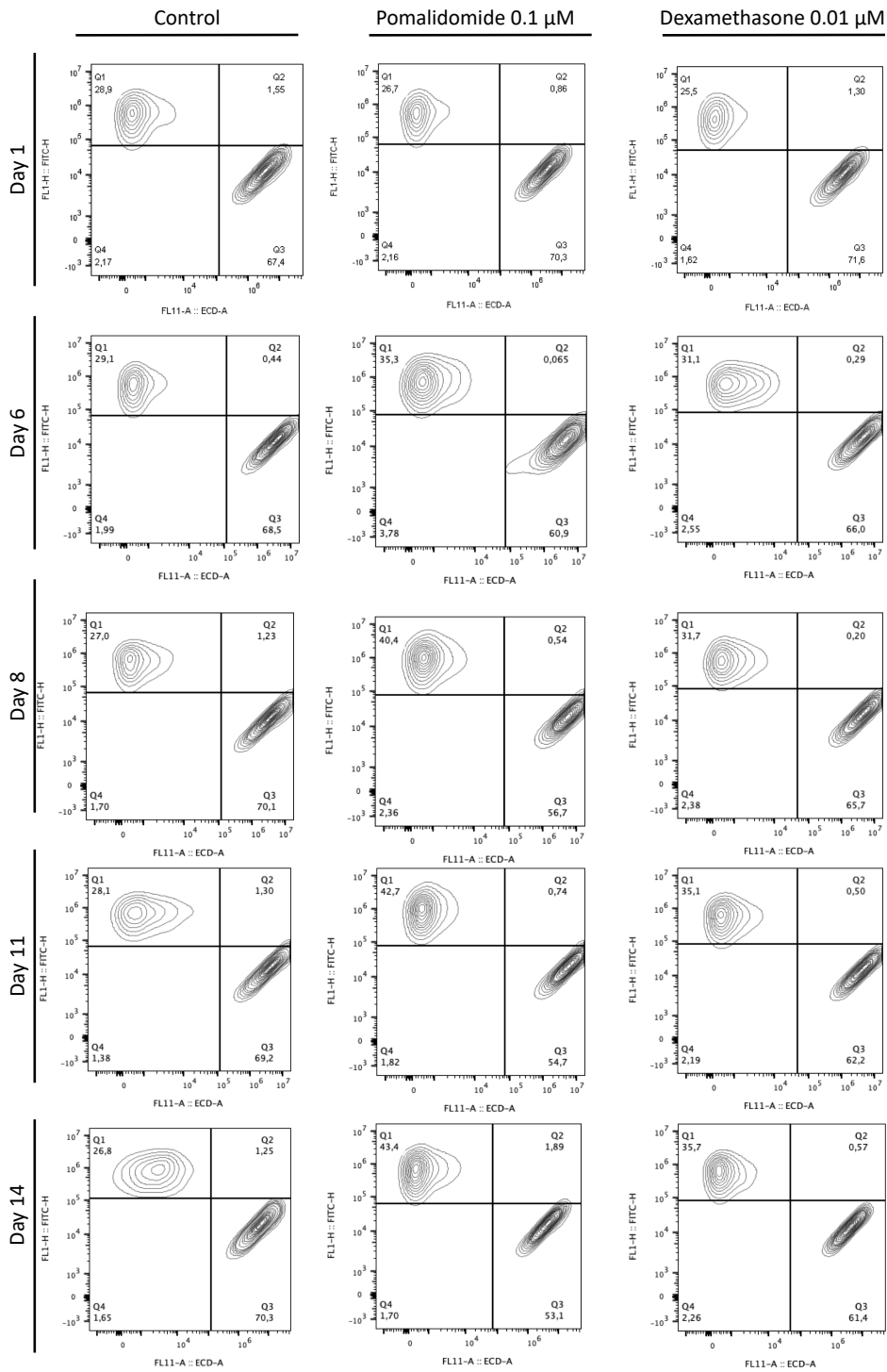
Figure S6: FACS analysis competition assay MM.1S BIRC3 KO. *Cells were gated for live cells prior to FITC-H and ECD-A analysis. Quadrant Q1 was deemed GFP-positive, and quadrant Q3 was deemed dTomato positive. Pomalidomide was added at 0.01 μM. Dexamethasone was added at 0.001 μM over 14 days. Control is DMSO.*
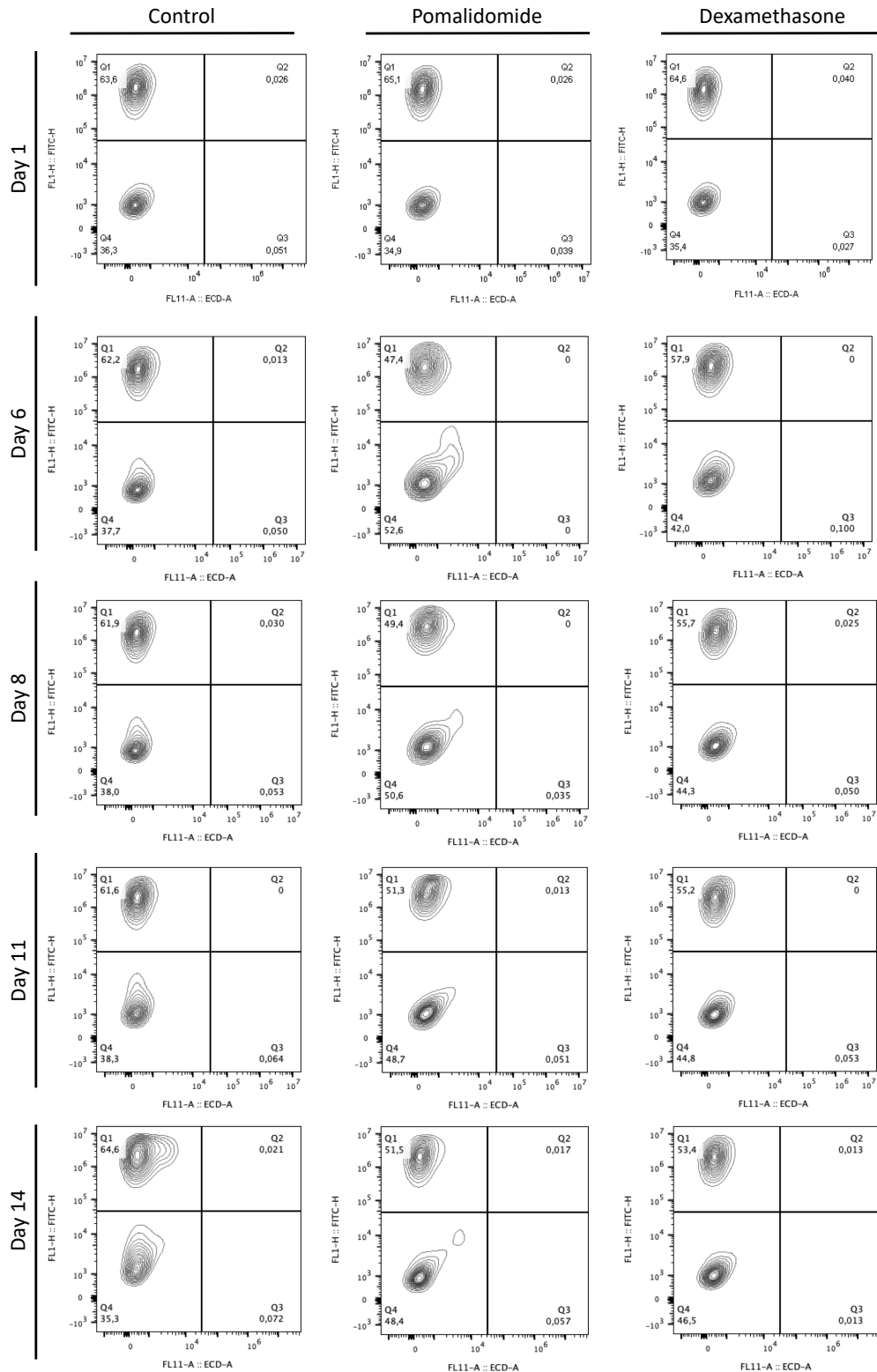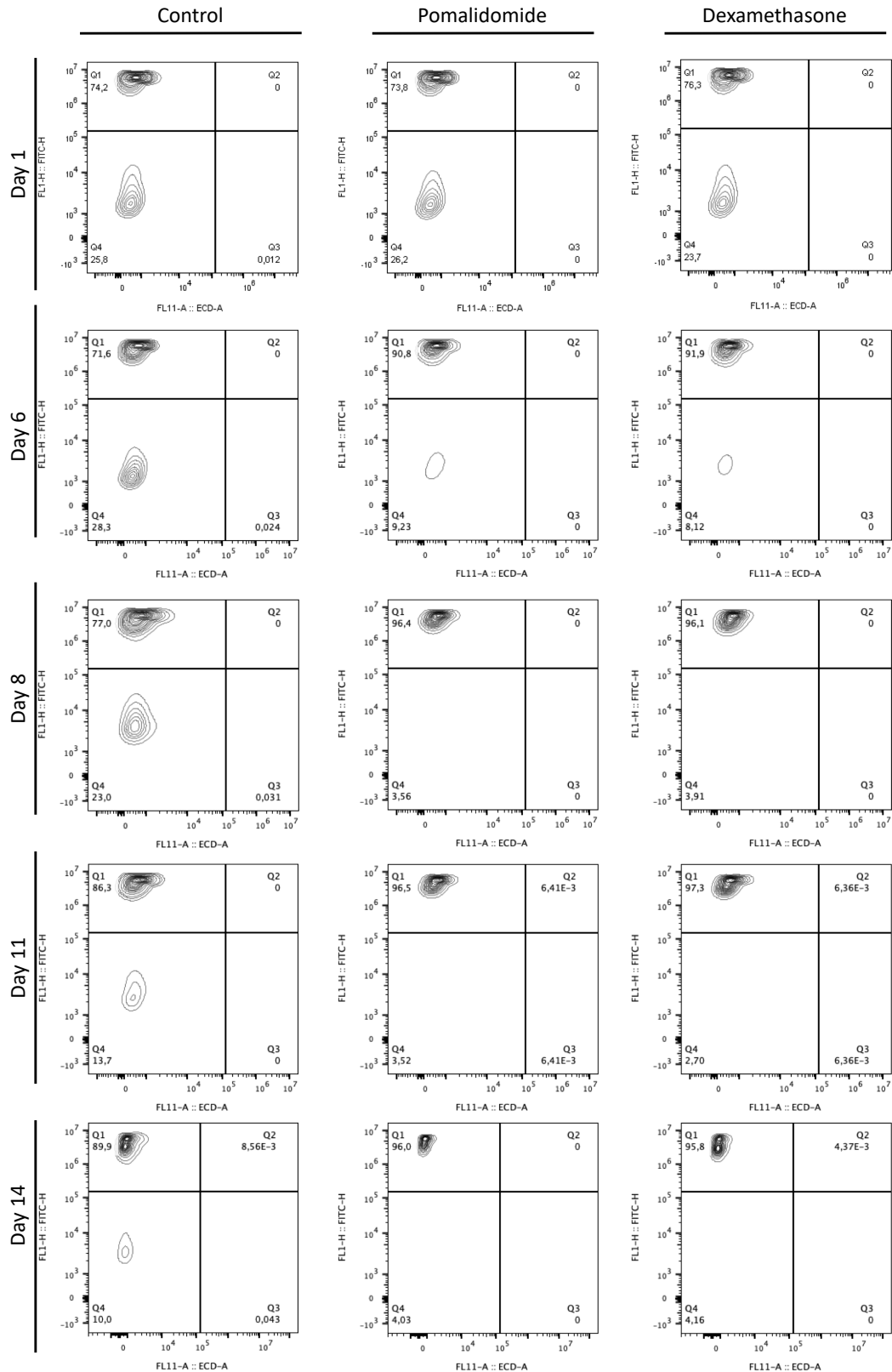
Figure S7: FACS analysis competition assay MM.1S XIAP KO. *Cells were gated for live cells prior to FITC-H and ECD-A analysis. Quadrant Q1 was deemed GFP-positive, and quadrant Q4 was deemed fluorescent negative (XIAP). Pomalidomide was added at 0.01 μM. Dexamethasone was added at 0.001 μM over 14 days. Control is DMSO.*

Figure S8: FACS analysis competition assay MM.1S CYLD KO. *Cells were gated for live cells prior to FITC-H and ECD-A analysis. Quadrant Q1 was deemed GFP-positive, and quadrant Q3 was deemed dTomato positive. Pomalidomide was added at 0.01 μM. Dexamethasone was added at 0.001 μM over 14 days. Control is DMSO.*
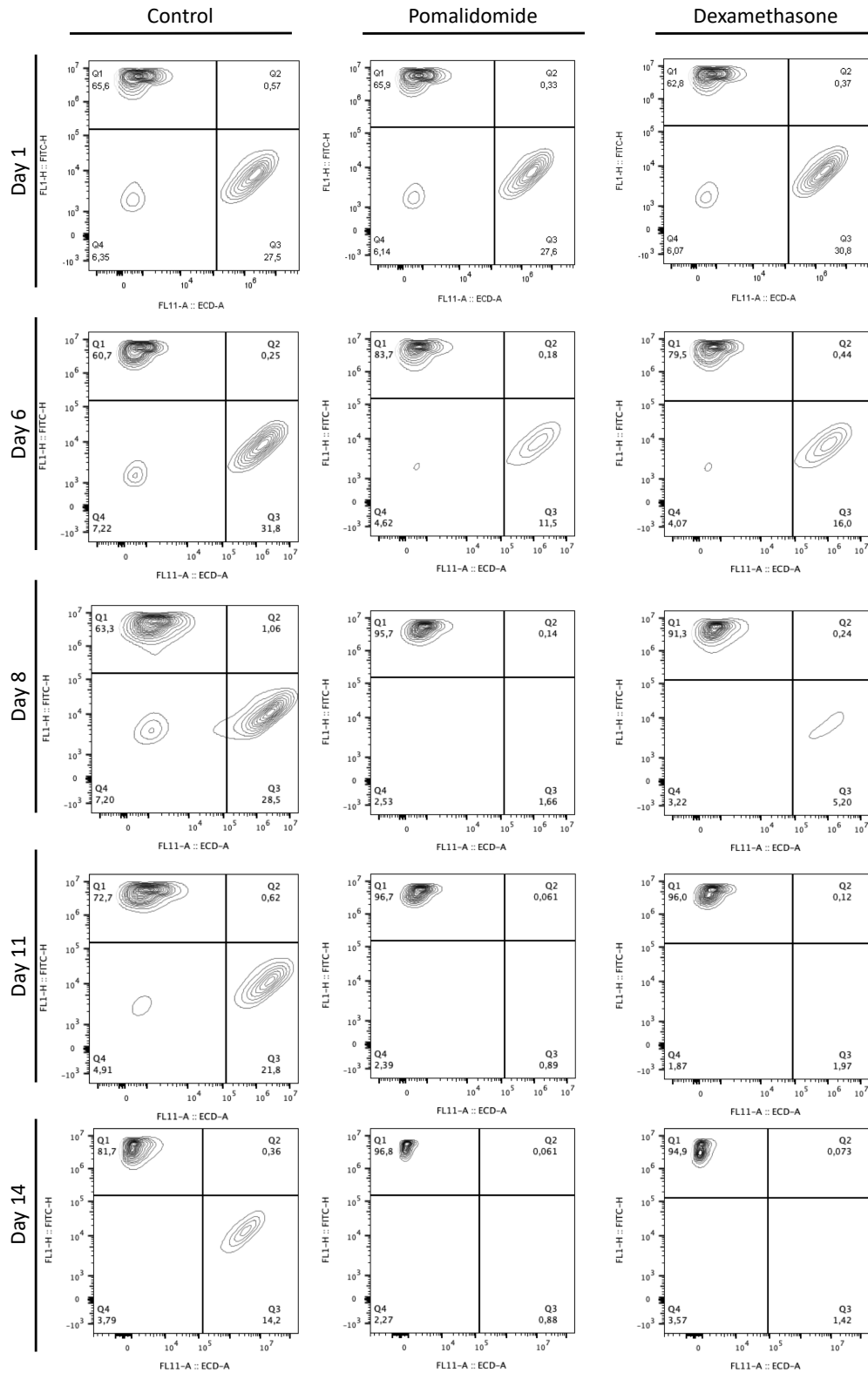
Figure S9: FACS analysis competition assay OPM2 Luciferase. *Cells were gated for live cells prior to FITC-H and ECD-A analysis. Quadrant Q1 was deemed GFP-positive, and quadrant Q3 was deemed dTomato positive. Pomalidomide was added at 0.01 μM. Dexamethasone was added at 0.001 μM over 14 days. Control is DMSO.*
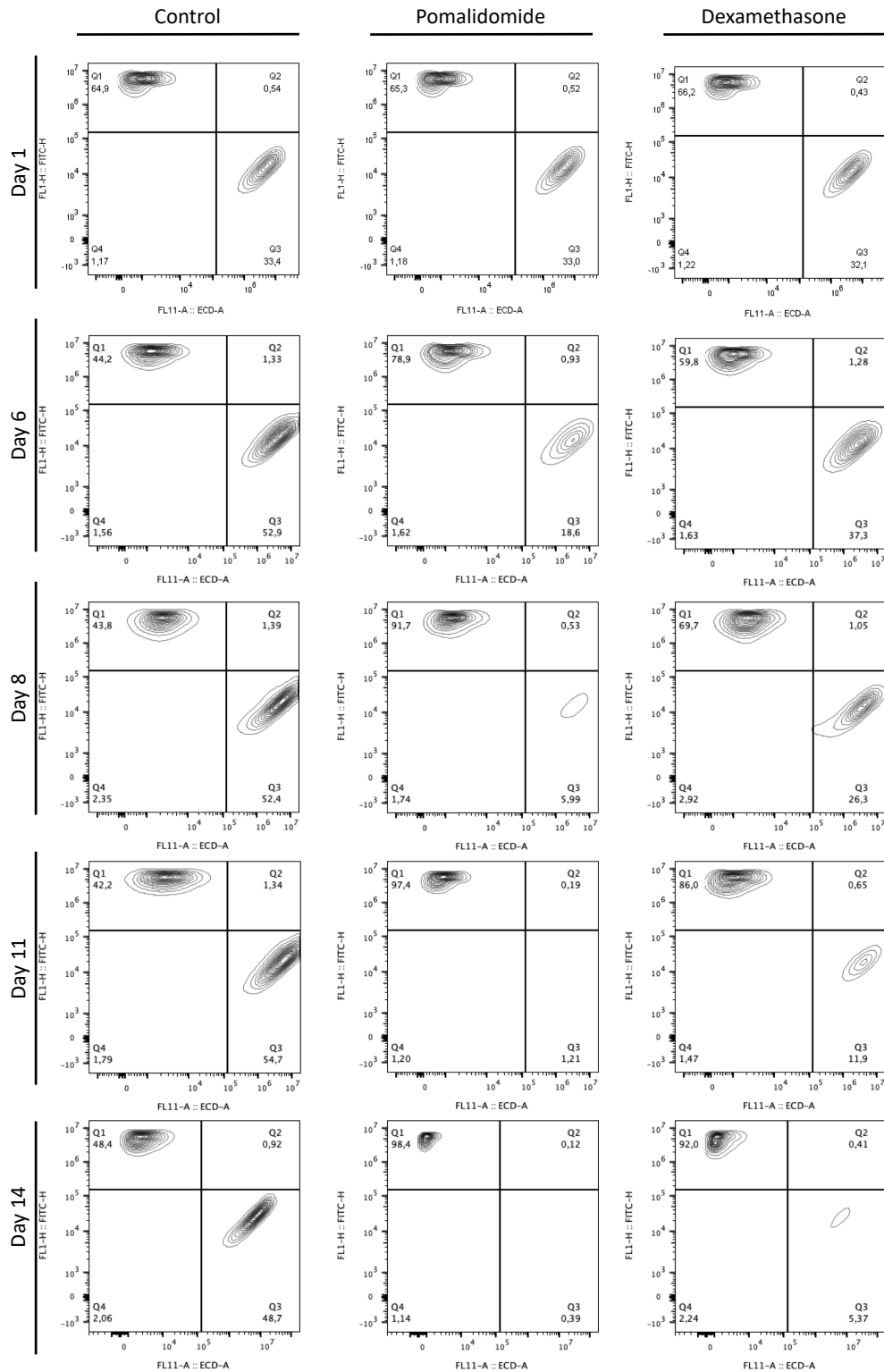
Figure S10: FACS analysis competition assay OPM2 BIRC2 KO. *Cells were gated for live cells prior to FITC-H and ECD-A analysis. Quadrant Q1 was deemed GFP-positive, and quadrant Q3 was deemed dTomato positive. Pomalidomide was added at 0.01 μM. Dexamethasone was added at 0.001 μM over 14 days. Control is DMSO.*

39

Figure S11: FACS analysis competition assay OPM2 XIAP KO. *Cells were gated for live cells prior to FITC-H and ECD-A analysis. Quadrant Q1 was deemed GFP-positive, and quadrant Q3 was deemed dTomato positive. Pomalidomide was added at 0.01 μM. Dexamethasone was added at 0.001 μM over 14 days. Control is DMSO.*

Figure S12: FACS analysis competition assay OPM2 CYLD KO. *Cells were gated for live cells prior to FITC-H and ECD-A analysis. Quadrant Q1 was deemed GFP-positive, and quadrant Q3 was deemed dTomato positive. Pomalidomide was added at 0.01 µM. Dexamethasone was added at 0.001 µM over 14 days. Control is DMSO.*

Figure S13: FACS analysis competition assay OPM2 TRAF3 KO. *Cells were gated for live cells prior to FITC-H and ECD-A analysis. Quadrant Q1 was deemed GFP-positive, and quadrant Q3 was deemed dTomato positive. Pomalidomide was added at 0.01 μM. Dexamethasone was added at 0.001 μM over 14 days. Control is DMSO.*